PROJECTE FINAL DE CARRERA

Study And Analysis Of An Optical OFDM Based On The Discrete Hartley Transform For IM/DD Systems

Estudis: Enginyeria de Telecomunicació

Autor: Fabiana Ferraro

Directora: Michela Svaluto Moreolo

Any: 2010

Index

Collaborations

Ringraziamenti

Giunta al termine di questa fase della mia vita vorrei ringraziare tutte le persone che, in modi diversi, hanno permesso e incoraggiato i miei studi e questa tesi:

grazie ai miei genitori, per il loro sostegno e appoggio: senza di voi non sarei potuta arrivare fin qui;

grazie a Davide, Simona e Camilla;

grazie a Fabio per l'aiuto, i consigli e tutto l'appoggio che non si può descrivere nei ringraziamenti di una tesi;

grazie al CTTC ed in particolar modo a Michela ed alla sua guida nello sviluppo, crescita e stesura di questa tesi;

grazie ai prof. Junyent, Carena e Poggiolini;

grazie a chiunque abbia inventato l'Erasmus;

grazie a Barcellona: te echarè mucho de menos;

grazie al Politecnico e alle creature che lo popolano;

grazie a Chiara, casa Vallirana, Ale, Arvin e Matte;

grazie a GigaCesca per tutti gli appunti;

grazie a Rena per l'aiuto tipografico;

grazie a tutti i miei amici;

grazie a tutti coloro che ho dimenticato di menzionare.

Abstract

Orthogonal frequency division multiplexing (OFDM) is used extensively in broadband wired and wireless communication systems because it is an effective solution to inter-symbol interference (ISI) caused by a dispersive channel. While many details of OFDM systems are very complex, the basic concept of OFDM is quite simple: data is transmitted in parallel on a number of different frequencies, and as a result the symbol period is much longer than for a serial system with the same total data rate. Because the symbol period is longer, ISI affects at most one symbol, and equalization is simplified. In most OFDM implementations any residual ISI is removed by using a form of guard interval called a cyclic prefix.

The application of OFDM to optical communications has only occurred very recently, but there are an increasing number of papers on the theoretical and practical performance of OFDM in many optical systems. In typical (non-optical) OFDM systems, the information is carried on the electrical field and the signal can have both positive and negative values (bipolar). At the receiver there is a local oscillator and coherent detection is used. In contrast, in a typical intensity-modulated direct-detection optical system,

the information is carried on the intensity of the optical signal and therefore can only be positive (unipolar).

In chapter 2, the Discrete multitone modulation (DMT) is presented. DMT is a baseband version of the better-known orthogonal frequency division multiplexing. DMT is a multicarrier modulation technique where a high-speed serial data stream is divided into multiple parallel lower-speed streams and modulated onto multiple subcarriers of different frequencies for simultaneous transmission.

Based on the fast Fourier transform (FFT) algorithm, multicarrier modulation and demodulation are efficiently implemented with DMT. Contrary to OFDM, the DMT modulator output signal after the inverse FFT ($IFFT$) is real-valued and no in-phase and quadrature (IQ-) modulation onto a radio frequency (RF) carrier is required.

Two forms of unipolar OFDM are proposed: DC-biased optical OFDM (DCO-OFDM) and asymmetrically clipped OFDM (ACO-OFDM). In DC-biased OFDM, a DC bias is added to the signal, however because of the large peak-to-average power ratio of OFDM, even with a large bias some negative peaks of the signal will be clipped and the resulting distortion limits performance. In ACO-OFDM the bipolar OFDM signal is clipped at the zero level: all negative going signals are removed. If only the odd frequency OFDM subcarriers are non zero at the IFFT input, all of the clipping noise falls on the even subcarriers, and the data carrying odd subcarriers are not impaired.

After a general overview, theoretical and simulation results are presented for the performance of asymmetrically-clipped optical OFDM and DC-biased optical OFDM using the Discrete Multitone Modulation in AWGN for intensity-modulated direct-detection systems. Constellations from 4 QAM to 1024 QAM are considered. For DCO-OFDM, the optimum bias depends on the constellation size which limits its performance in adaptive systems. ACO-OFDM requires less optical power for a given data rate than DCO-

OFDM and is better suited to adaptive systems as the same structure is optimum for all constellations.

In chapter 3 a novel power-efficient optical OFMD based on the Discrete Hartley Transform is presented. Hartley transform is particularly attractive for the processing of real signals because the direct and inverse transforms are identical, and the Hartley transform of a real signal is real. Will be demonstrate that asymmetrically clipping (AC) technique can also be applied to DHT-based OFDM; the signal can be transmitted without the need of a DC bias, resulting in a power-efficient system, not affected by clipping noise. Hermitian symmetry is not required for the input signal. Therefore, this technique supports the double of input symbols compared to both AC and DC-biased O-OFDM, based on standard Fourier processing. The analysis in an additive white Gaussian noise channel shows that the same performance can be achieved by replacing 4-QAM (quadrature-amplitude modulation) optical-OFDM with a simpler system based on DHT, using binary phase-shift keying (BPSK).

In chapter 4 simulations of all the previous results are presented using VPIsystems' VPItransmissionMaker™ V8.5.

CHAPTER 1
Introduction to OFDM

Orthogonal frequency division multiplexing (OFDM) is used extensively in broadband wired and wireless communication systems because it is an effective solution to inter-symbol interference (ISI) caused by a dispersive channel. This becomes increasingly important as data rates increase to the point where, when conventional serial modulation schemes like quadrature amplitude modulation (QAM) or NRZ are used, the received signal at any time depends on multiple transmitted symbols. In this case the complexity of equalization in serial schemes which use time domain equalization rises rapidly. In contrast, the complexity of OFDM, and of systems using serial modulation and frequency domain equalization, scale well as data rates and dispersion increase. A second major advantage of OFDM is that it transfers the complexity of transmitters and receivers from the analog to the digital domain. For example, while the precise design of analog filters can have a major impact on the performance of serial modulation systems, in OFDM any phase variation with frequency can be corrected at little or no cost in the digital parts of the receiver. Despite

these important advantages of OFDM, it is only recently that it has been considered for optical communications.

While many details of OFDM systems are very complex, the basic concept of OFDM is quite simple: data is transmitted in parallel on a number of different frequencies, and as a result the symbol period is much longer than for a serial system with the same total data rate. Because the symbol period is longer, ISI affects at most one symbol, and equalization is simplified. In most OFDM implementations any residual ISI is removed by using a form of guard interval called a cyclic prefix.

When frequency division multiplexing (FDM) is used in conventional wireless systems, or wavelength division multiplexing (WDM) is used in optical systems, information is also transmitted on a number of different frequencies simultaneously.

However there are a number of key theoretical and practical differences between OFDM and these conventional systems:

- in OFDM the subcarrier frequencies are chosen so that the signals are mathematically orthogonal over one OFDM symbol period.
- both modulation and multiplexing are achieved digitally using an inverse fast Fourier transform (IFFT) and as a result, the required orthogonal signals can be generated precisely and in a very computationally efficient way.

In FDM/WDM there are frequency guard bands between the subcarriers. At the receiver the individual subcarriers are recovered using analog filtering techniques. In OFDM the spectra of individual subcarriers overlap, but because of the orthogonality property, as long as the channel is linear, the subcarriers can be demodulated without interference and without the need for analog filtering to separate the received subcarriers.

Demodulation and demultiplexing is performed by a fast Fourier transform (FFT).

The spectrum of an individual OFDM subcarrier has a form, so each OFDM subcarrier has significant sidelobes over a frequency range which includes

many other subcarriers. This is the cause of one of the major disadvantages of OFDM: that it is quite sensitive to frequency offset and phase noise.

Fig. 1 shows spectra for FDM/WDM and OFDM.

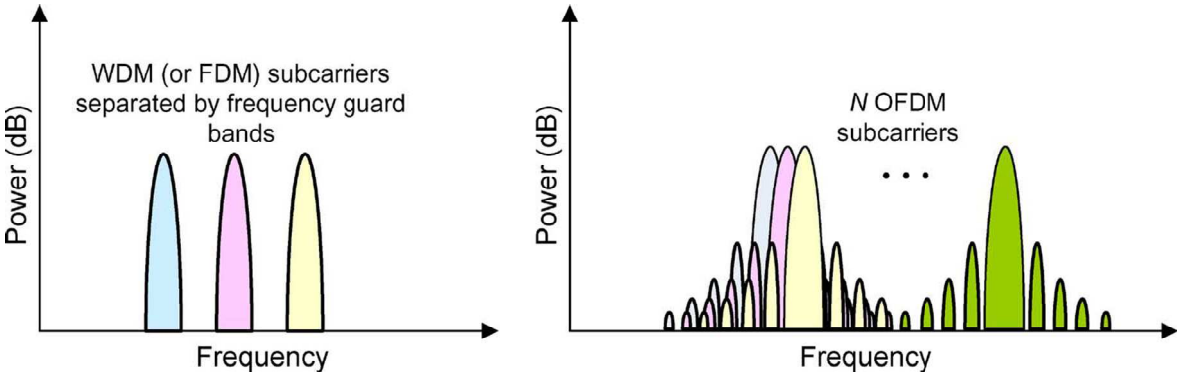

Fig. 1.1 Spectra for WDM and OFDM

1.1 History

The first proposal to use orthogonal frequencies for transmission appears in a 1966 patent by Chang of Bell Labs [13]. The proposal to generate the orthogonal signals using an FFT came in 1969 [14]. The cyclic prefix (CP), which is an important aspect of almost all practical OFDM implementations, was proposed in 1980 [15]. These are the three key aspects that form the basis of most OFDM systems.

OFDM began to be considered for practical wireless applications in the mid–1980s. Cimini of Bell Labs published a paper on OFDM for mobile communications in 1985 [16], while in 1987, Lassalle and Alard, [17] considered the use of OFDM for radio broadcasting and noted the importance of combining forward error correction (FEC) with OFDM. Because of this interrelationship, OFDM is often called Coded OFDM (C-OFDM) by broadcast engineers. The application of OFDM for wireline communications was pioneered by Cioffi and others at Stanford who demonstrated its potential as a modulation technique for digital subscriber

loop (DSL) applications [1]. OFDM is now the basis of many practical telecommunications standards including wireless local area networks (LAN), fixed wireless and television and radio broadcasting in much of the world [18]. OFDM is also the basis of most DSL standards, though in DSL applications the baseband signal is not modulated onto a carrier frequency and in this context OFDM is usually called discrete multitone (DMT).
The application of OFDM to optical communications has only occurred very recently, but there are an increasing number of papers on the theoretical and practical performance of OFDM in many optical systems.

1.2 OFDM system for wireless applications

In this section the basic functions of a typical OFDM system for wireless applications are described. Fig. 1.2 shows the block diagram of the transmitter and receiver of a typical OFDM wireless system.

1.2.1. Coding Interleaving and Mapping

The first blocks in the transmitter are interleaving and coding. All OFDM systems use some form of error correction or detection because, if there is frequency selective fading in the channel, some of the parallel data streams will experience deep fading. The coding is usually preceded by interleaving because a number of adjacent OFDM subcarriers may fall within the frequencies which are experiencing fading. In most broadcast applications of OFDM such as digital audio broadcasting (DAB) and digital video broadcasting (DVB) there are two layers of interleaving and coding so that a very low overall bit error rate (BER) can be achieved even over a very noisy channel. After coding, the data is mapped onto complex numbers representing the QAM constellation being used for transmission. Constellation sizes from 4 QAM to 64 QAM are typically used. While phase shift keying (PSK) is compatible with OFDM, it is rarely used. PSK in

OFDM, unlike PSK in single carrier systems, does not have a constant signal envelope and, for large constellations, has smaller distance between constellation points and so is more susceptible to noise. The sequence of complex numbers output from the constellation mapping are then serial-to-parallel (S/P) converted to form a vector suitable for input to the $IFFT$.

1.2.2 FFT and IFFT

The IFFT block is the main component in the transmitter and the FFT in the receiver, and these are the functions which distinguish OFDM from single carrier systems.

The input to the IFFT is the complex vector $\boldsymbol{X} = [\, X_0 \;\; X_1 \;\; X_2 \;\; \ldots \;\; X_{N-1} \,]^T$, the vector has length N where N is the size of the $IFFT$. Each of the elements of $\boldsymbol{X}$ represents the data to be carried on the corresponding subcarrier. Usually QAM modulation is used in OFDM, so each of the elements of $\boldsymbol{X}$ is a complex number representing a particular QAM constellation point. The output of the IFFT is the complex vector

$\boldsymbol{x} = [\, x_0 \;\; x_1 \;\; x_2 \;\; \ldots \;\; x_{N-1} \,]^T$ Using the definition of the inverse discrete Fourier transform:

$$x_m = \frac{1}{\sqrt{N}} \sum_{k=0}^{N-1} X_k \exp\left(\frac{j2\pi km}{N}\right) \qquad \text{for } 0 \le m \le N-1 \qquad (1.1)$$

The forward FFT corresponding to (1) is

$$X_k = \frac{1}{\sqrt{N}} \sum_{m=0}^{N-1} x_m \exp\left(\frac{-j2\pi km}{N}\right) \qquad \text{for } 0 \le k \le N-1 \qquad (1.2)$$

This form of the $IFFT/FFT$ transform pair has the important advantage that the discrete signals at the input and the output of the transform for each symbol have the same total energy and the same average power. This simplifies the analysis of many OFDM functions. While the components of

$\boldsymbol{X}$ take only a few discrete values, the probability distribution of $\boldsymbol{x}$ is not obvious.

In fact for $N \geq 64$ the real and imaginary components of an OFDM time domain signal are approximately Gaussian. For wireless OFDM systems which have already been standardized, values of N ranging from 64 in wireless LAN systems to 8096 in digital television systems have been used [18].

At the receiver the FFT performs a forward transform on the received sampled data for each symbol

$$Y_k = \frac{1}{\sqrt{N}} \sum_{m=0}^{N-1} y_m \exp\left(\frac{-j2\pi km}{N}\right) \qquad \text{for } 0 \leq k \leq N-1 \qquad (1.3)$$

where $\boldsymbol{y} = [\, y_0 \;\; y_1 \;\; y_2 \;\; \dots \;\; y_{N-1} \,]^T$ is the vector representing the sampled time domain signal at the input to the receiver FFT and $\boldsymbol{Y} = [\, Y_0 \;\; Y_1 \;\; Y_2 \;\; \dots \;\; Y_{N-1} \,]^T$ is the discrete frequency domain vector at the FFT output. Note that only N samples are required per OFDM symbol (excluding CP). To understand the function of the $IFFT$, first consider what would happen if there were no noise or distortion in the channel or the transmitter and receiver front ends, then because the FFT and $IFFT$ are transform pairs, $\boldsymbol{X} = \boldsymbol{Y}$.

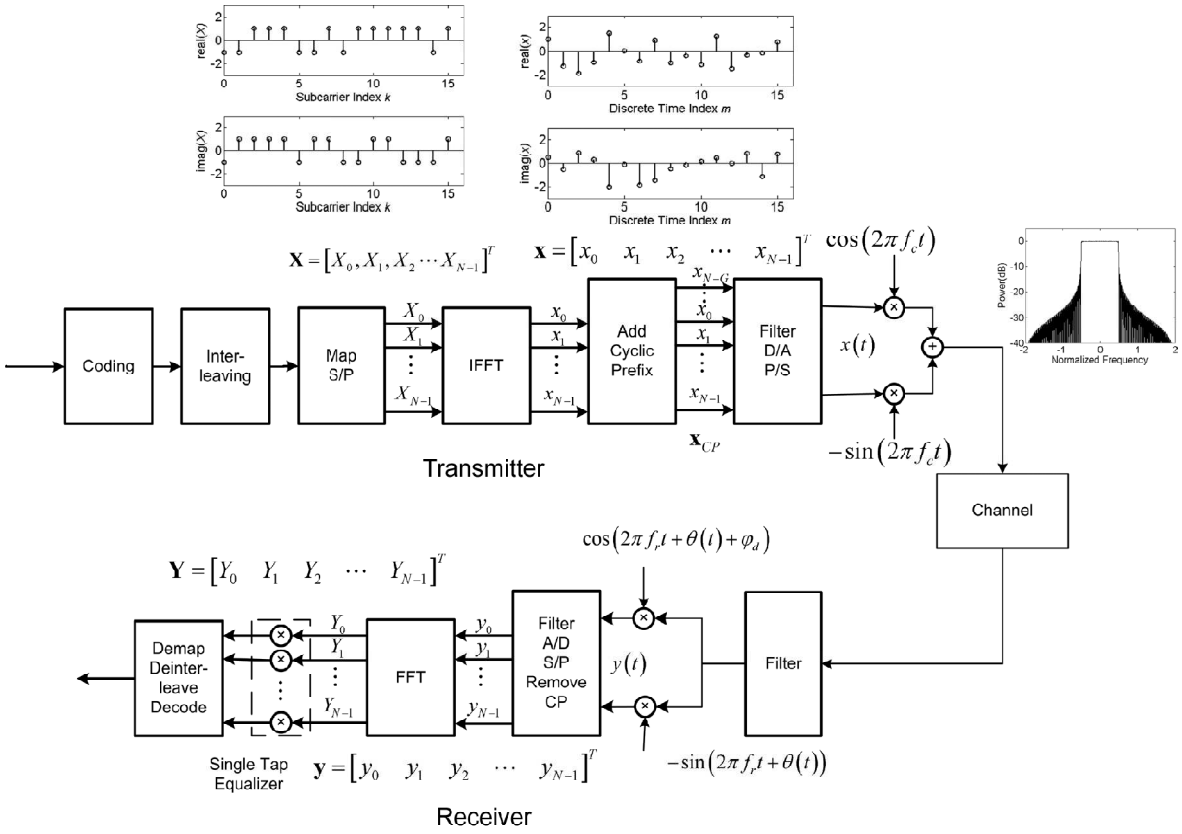

Fig. 1.2 Block diagram of an OFDM communication system for RF wireless applications.

If additive white Gaussian noise (AWGN) is added to the signal, but the signal is not distorted then

$$y_m = x_m + w_m \tag{1.4}$$

Where w_m is a sample of white Gaussian noise, substituting (1.4) in (1.3) and rearranging gives

$$Y_k = \frac{1}{\sqrt{N}} \sum_{m=0}^{N-1} y_m \exp\left(\frac{-j2\pi km}{N}\right) = X_k + W_k \tag{1.5}$$

where

$$W_k = \frac{1}{\sqrt{N}} \sum_{m=0}^{N-1} y_m \exp\left(\frac{-j2\pi km}{N}\right) \qquad for\ 0 \leq k \leq N-1 \tag{1.6}$$

W_k is the noise component of the kth output of the receiver FFT. Because each value of W_k is the summation of N independent white Gaussian noise samples, w_m, it is an independent white Gaussian noise process too. Even

if the time domain noise, w_m, does not have a Gaussian distribution, in most cases, because of the central limit theorem, the frequency domain noise W_k will be Gaussian. This, combined with the use of FEC, means that usually the performance of OFDM systems depend on the average noise power, unlike conventional serial optical systems where it is the peak values of the noise which often limit performance.

1.2.3 Sequences of Symbols and the Cyclic Prefix

The description above showed how the $IFFT$ generates each OFDM symbol. The transmitted signal consists of a sequence of these OFDM symbols. To denote different OFDM symbols when a sequence of symbols rather than a single symbol is being considered, it is necessary to extend the notation to include a time index. Let $\boldsymbol{x}(i) = [x_0(i)\ x_1(i)\ x_2(i) \dots x_{N-1}(i)]^T$ be the output of the $IFFT$ in the ith symbol period. In most OFDM systems, a CP is added to the start of each time domain OFDM symbol before transmission. In other words a number of samples from the end of the symbol is appended to the start of the symbol. So instead of transmitting

$$\boldsymbol{x}(i) = [x_0(i)\ x_1(i)\ x_2(i) \dots x_{N-1}(i)]^T$$

the sequence

$$\boldsymbol{x}_{CP}(i) = [x_{N-G}(i) \dots x_{N-1}(i), \quad x_0(i) \dots x_{N-1}(i)]^T \qquad (1.7)$$

is transmitted; where G is the length of the cyclic prefix. Although the CP introduces some redundancy, and reduces the overall data rate, it was shown that the use of the CP eliminates both ISI and inter-carrier interference (ICI) from the received signal and is the key to simple equalization in OFDM.

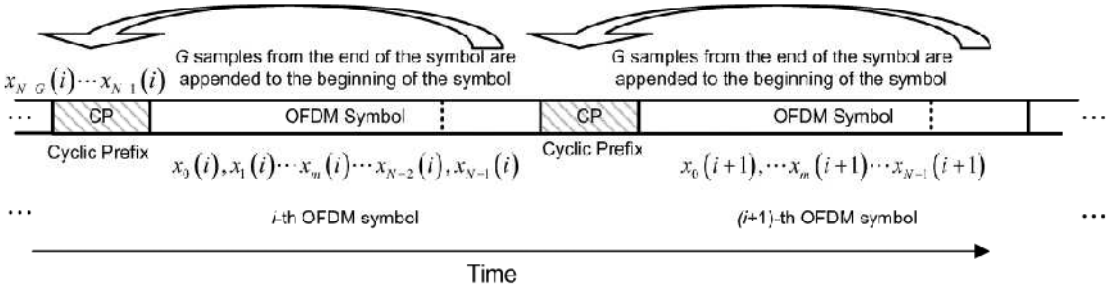

Fig. 1.3 Time domain sequence of OFDM symbols showing the cyclic prefix.

1.2.4 Individual OFDM Subcarriers

Considerable insight into the operation of an OFDM system can be obtained by considering what happens to individual subcarriers as they pass through the system. However, it is also important to note that in an OFDM system because the $IFFT$ simultaneously performs modulation and multiplexing there is no point in the transmitter or receiver where an individual time domain subcarrier can be observed. Individual subcarriers are present only in the frequency domain. Nevertheless consideration of the time domain components due to individual subcarriers is important, and if the channel is linear the performance of the overall system can be derived in this way. To simplify the discussion we will not at first consider the CP and will consider only one symbol.

From (1.1), the discrete time domain component associated with the kth subcarrier of a given OFDM symbol is

$$x_m = \frac{1}{\sqrt{N}} X_k \exp\left(\frac{j2\pi km}{N}\right) \qquad \text{for } 0 \le m \le N-1 \qquad (1.8)$$

1.2.5 OFDM in a Dispersive Environment

OFDM is so widely used because, when a CP is used, any distortion caused by a linear dispersive channel can be corrected simply using a 'single-tap' equalizer. To understand why this is true, consider a simple case where there is perfect up-conversion and down-conversion, but where the

received baseband signal is the sum of two versions of the transmitted signal with different gains and delay.

$$y(t) = g_1 x(t + \tau_1) + g_2 x(t + \tau_2) \qquad (1.9)$$

For the case where OFDM transmission is at passband, the gains and the signals will be complex; for the case of baseband transmission the gains and signals are real.

Fig. 1.3 shows two delayed versions of an OFDM signal and the time window for the receiver FFT. For each OFDM symbol the receiver FFT has as input samples from the signal within the time period shown. From Fig. 1.3 it can be seen that as long as the start of the receiver time window is aligned with the start of the "main" OFDM symbol of the first arriving signal, and if the delay spread is less than the length of the CP, there is no inter-symbol interference. The signal received in the ith time window depends only on the ith transmitted symbol.

Inter-symbol interference could also be eliminated by preceding each OFDM symbol with a guard interval in which no signal was transmitted, however this would result in a phenomenon called inter-carrier interference (ICI). Each value of Y_k would depend on input values $\boldsymbol{X}$ other than X_k. When a CP is used, each OFDM subcarrier is represented by a continuous sinusoid of the appropriate frequency throughout the main symbol period and the associated CP.

Now consider analytically the effect of a dispersive channel on a single subcarrier. To simplify the discussion we will consider a subcarrier in the range $0 \leq k \leq N/2 - 1$ and ignore the effect of noise.

Let the continuous baseband signal at the transmitter associated with the kth subcarrier of a given OFDM symbol (including the CP) be

$$x(k,t) = \frac{1}{\sqrt{N}} X_k \exp\left(\frac{j2\pi kt}{T}\right) \qquad \text{for } 0 \leq k \leq \frac{N}{2} - 1 \qquad (1.10)$$

Then the received continuous time domain signal for the two path channel described in (9) is

$$y(k,t) = \frac{1}{\sqrt{N}} g_1 X_k \exp\left(\frac{j2\pi k(t-\tau_1)}{T}\right) + \frac{1}{\sqrt{N}} g_2 X_k \exp\left(\frac{j2\pi k(t-\tau_2)}{T}\right)$$
$$for\ 0 \le k \le \frac{N}{2} - 1 \quad (1.11)$$

Ideally the receiver should be synchronized so that the FFT window is aligned with the start of the main symbol period for the first arriving version of the transmitted signal. So for this case the receiver FFT window should be offset by τ_1. In this case

$$y(k,t) = \frac{1}{\sqrt{N}} g_1 X_k \exp\left(\frac{j2\pi kt}{T}\right) + \frac{1}{\sqrt{N}} g_2 X_k \exp\left(\frac{j2\pi k(t-(\tau_2-\tau_1))}{T}\right)$$
$$= \frac{1}{\sqrt{N}} g_1 X_k \exp\left(\frac{j2\pi kt}{T}\right) \times \left(g_1 + g_2 \exp\left(\frac{-j2\pi k(\tau_2-\tau_1)}{T}\right)\right) \quad (1.12)$$

So after demodulation by the FFT and including the effect of noise

$$Y_k = X_k \left(g_1 + g_2 \exp\left(\frac{-j2\pi k(\tau_2-\tau_1)}{T}\right)\right) + W_k = H_k X_k + W_k \quad (1.13)$$

Where

$$H_k = g_1 + g_2 \exp\left(\frac{-j2\pi k(\tau_2-\tau_1)}{T}\right) \quad (1.14)$$

The transmitted data can be recovered from the received signal by multiplying X_k by $1/H_k$. That is: each subcarrier can be recovered using one complex multiplication.

1.2.6 Transmitter and Receiver Front End

The remaining section of the transmitter is the front end. Fig. 1.2 shows a block combining filtering, parallel-to-serial conversion (P/S) and digital-to-analog conversion (D/A) because in practice there is some choice about the order of these processes.

For example, OFDM symbols are often windowed (a form of time variant filtering) to reduce the side lobes, sometimes the digital signal is up-sampled before D/A conversion to simplify the analog filtering, and

filtering can be in the analog or digital domain. However after this process the signal $x(t)$ is an approximately band-limited signal consisting of sinusoids of the baseband subcarrier frequencies. In wireless OFDM systems $x(t)$ is a complex signal which forms the input to an IQ modulator for up-conversion to the carrier frequency. In baseband systems such as ADSL, $x(t)$ is a real signal. In these systems, $\boldsymbol{X}$, the input to the transmitter $IFFT$ is constrained to have Hermitian symmetry; $X_{N-1} = X_k^*$ where * denote complex conjugation. This results in the imaginary components of the $IFFT$ outputs canceling.

At the receiver, in wireless systems the signal is down-converted by mixing with in-phase and quadrature components of a locally generated carrier,$\cos(2\pi f_r t + \theta(t) + \varphi_d)$ and$-\sin(2\pi f_r t + \theta(t))$. Ideally the frequency of the local carrier, f_r, is identical to the carrier frequency of the received signal, but in practice there may be some difference. This can be caused by error in the carrier recovery at the receiver, or in wireless systems, by Doppler effects due to moving transmitter, receiver or reflectors.

Typical OFDM System	Bipolar	Information carried on electrical field	Local Oscillator receiver	Cohererent Reception
Typical Optical System	Unipolar	Information carried on optical intensity	No local Oscillator (laser) al receiver	Direct Detection

Table 1.1 Comparison of typical ofdm system and typical optical system

1.3 OFDM for optical communications

Despite the many advantages of OFDM, and its widespread use in wireless communications, OFDM has only recently been applied to optical communications. This is partly because of the recent demand for increased data rates across dispersive optical media and partly because

developments in digital signal processing (DSP) technology make processing at optical data rates feasible. However another important obstacle has been the fundamental differences between conventional OFDM systems and conventional optical systems. Table 1.1 summarizes these differences.

In typical (non-optical) OFDM systems, the information is carried on the electrical field and the signal can have both positive and negative values (bipolar). At the receiver there is a local oscillator and coherent detection is used. In contrast in a typical intensity-modulated direct-detection optical system, the information is carried on the intensity of the optical signal and therefore can only be positive (unipolar). There is no laser at the receiver acting as a local oscillator and direct detection rather than coherent detection is used. A variety of optical OFDM solutions have been proposed for different applications. To understand these different techniques, it is useful to realize what is fundamental in each domain. For an OFDM system to work successfully the system must be (approximately) linear between the transmitter IFFT input and the receiver FFT output. In the optical domain, optical receivers use square-law detectors.

Optical OFDM solutions comprise techniques for systems where many different optical modes are received, for example, optical wireless, multimode fiber systems and plastic optical fiber systems. For these the OFDM signal should be represented by the intensity of the optical signal.

Optical OFDM Using Intensity Modulation

In [19], Kahn and Barry explain why the many optical modes that are present at the receiver result in optical wireless systems being linear in intensity. So, for optical wireless systems and other systems where many modes are received, the OFDM signal must be represented as intensity. This means that the modulating signal must be both real and positive, whereas baseband OFDM signals are generally complex and bipolar. A real baseband signal OFDM signal can be generated by constraining to have

Hermitian symmetry. Two forms of unipolar OFDM have been proposed: DC-biased optical OFDM (DCO-OFDM) and asymmetrically clipped OFDM (ACO-OFDM) [2], [3]. In DC-biased OFDM, a DC bias is added to the signal, however because of the large peak-to-average power ratio of OFDM, even with a large bias some negative peaks of the signal will be clipped and the resulting distortion limits performance [3]. In ACO-OFDM the bipolar OFDM signal is clipped at the zero level: all negative going signals are removed. If only the odd frequency OFDM subcarriers are non zero at the IFFT input, all of the clipping noise falls on the even subcarriers, and the data carrying odd subcarriers are not impaired [2]. In [3] it was shown that except for extremely large constellations ACO-OFDM requires a lower average optical power for a given BER and data rate than DCO-OFDM. ACO-OFDM has also been shown to be efficient from an information theoretic perspective [4]. The use of DCO-OFDM has been demonstrated experimentally for optical wireless [20], multimode fiber [5] and plastic optical fiber [21].

1.4 Disadvantages of OFDM

As well as its many advantages, OFDM has a number of disadvantages, of these the most important in wireless communications are the high peak-to-average power ratio (PAPR) and the sensitivity to phase noise and frequency offset.

1.4.1 Peak-to-Average Power Ratio

The high PAPR of OFDM means that if the signal is not to be distorted, many of components in the transmitter and receiver must have a wide dynamic range. In particular the output amplifier of the transmitter must be very linear over a wide range of signal levels. In wireless systems the expense and power consumption of these amplifiers is often an important

design constraint. Inter-modulation resulting from any nonlinearity results in two major impairments: out-of-band (OOB) power and in-band distortion. In wireless communications OOB power is usually the more important, because of the near-far problem; interference from the OOB power of a close transmitter may swamp reception from a distant transmitter. For this reason the specifications on OOB power in wireless are very stringent. OOB power caused by transmitter nonlinearities may be much less of a problem in optical applications of OFDM. In-band distortion is a relatively small effect and becomes important only for large signal constellations.

Solutions to the PAPR Problem

There are numerous papers describing different solutions to the PAPR problem. These can be broadly classified into techniques involving coding, techniques involving multiple signal representation (MSR), and techniques involving non linear distortion, such as clipping.

Coding techniques aim to apply coding to the input vector $\boldsymbol{X}$ so that OFDM symbols which have high PAPR are not used. Despite extensive research, effective codes have not been developed.

MSR involves generating a number of possible transmit signals for each input data sequence and using the one with the lowest PAPR.

To be an effective solution to PAPR, clipping must be performed on either the analog signal, or an up-sampled version of the digital signal with an oversampling factor of at least two. This is because once the signal is D/A converted the peaks of the signal may occur between the discrete samples.

1.4.2 Sensitivity to Frequency Offset, Phase Noise, and I/Q Imbalance

Differences in the frequency and phase of the receiver local oscillator and the carrier of the received signal can degrade system performance. In the existing OFDM literature these impairments are usually classified in terms of their source, for example, frequency offset between transmitter and receiver local oscillator [22], Doppler spread in the channel [23], and a variety of phase noise models with characteristics that depend on the mechanisms of carrier recovery in the receiver [24].

These results are in general not directly applicable to optical applications of OFDM. The effect of phase and frequency errors in terms of the relationship between the time variation of phase and its effect on the received constellation and how easily these errors can be corrected in the digital domain will be discuss.

First consider the case where there is no noise or distortion in the channel, and $\varphi_d = 0$ so that there is no I/Q phase imbalance. Then using the formulae for sums and products of angles and with simple manipulation, the time domain received signal samples are given by

$$y_m = x_m exp(j\theta_m) \qquad (1.15)$$

where θ_m is the phase error at the receiver for the mth sample of the OFDM symbol under consideration.

For the case where there is a constant phase error, $\theta_m = \theta_0$. Then $y_m = x_m exp(j\theta_0)$ and it is simple to show that

$$Y_k = exp(j\theta_0)X_k \qquad (1.16)$$

The constellation is simply rotated by angle θ_0. An example is shown in figure 1.4.

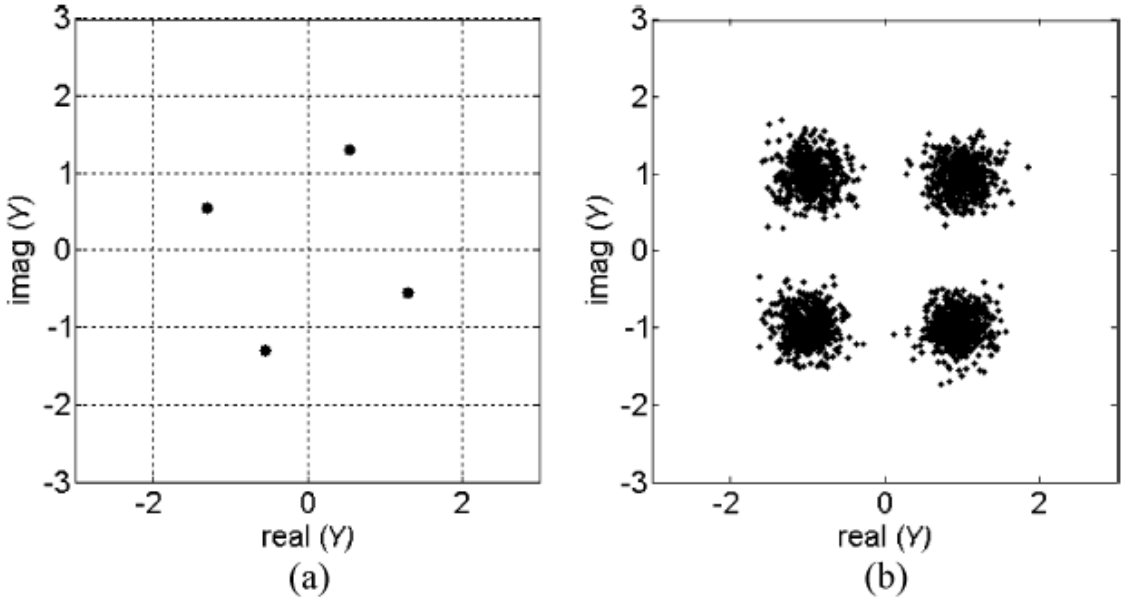

Fig 1.4 Effect of phase error on received OFDM constellation (a) when the phase error is constant and (b) when phase noise is uncorrelated

In an OFDM system, this would be automatically corrected in the single tap equalizer.

Now consider the opposite extreme, where the phase noise is zero mean, and there is no correlation between phase noise samples $E\{\theta_m\theta_n\} = 0\ for\ m \neq n$, where $E\{\ \ \}$ denotes the expectation operator.

Then taking the FFT gives

$$Y_k = \frac{1}{\sqrt{N}}\sum_{m=0}^{N-1} y_m \exp\left(\frac{-j2\pi km}{N}\right)$$
$$= \frac{1}{\sqrt{N}}\sum_{m=0}^{N-1} x_m \exp(j\theta_m) \exp\left(\frac{-j2\pi km}{N}\right) \qquad (1.17)$$

If the phase error is small, then using the small angle approximation $\exp(j\theta_m) \approx 1 + \theta_m$

$$Y_k = \frac{1}{\sqrt{N}}\sum_{m=0}^{N-1} x_m\,(1 + j\theta_m) \exp\left(\frac{-j2\pi km}{N}\right)$$

$$= X_k + \frac{1}{\sqrt{N}} \sum_{m=0}^{N-1} j\theta_m x_m \exp\left(\frac{-j2\pi km}{N}\right)$$

$$= X_k + N_k \qquad (1.18)$$

The demodulated subcarrier Y_k is equal to the transmitted subcarrier plus a noise like term, N_k, which depends on all of the transmitted subcarriers. The power of N_k can be calculated by using the fact that θ_m and x_m are statistically independent.

For θ_m with characteristics between these extremes, phase error results in a combination of the noise like ICI and constellation rotation (usually called "common phase error" in the literature).

CHAPTER 2
Discrete Multitone Modulation

Discrete multitone modulation (DMT) is a baseband version of the better-known orthogonal frequency division multiplexing (OFDM). While OFDM is known for its mass-application in Wireless Fidelity (WiFi) or wireless local area networks (WLAN) and terrestrial digital video broadcasting (DVB-T), DMT is widely employed in copper-based digital subscriber lines (DSL) for providing high-speed Internet access via asymmetric DSL (ADSL) and very high speed DSL (VDSL).

2.1 Principle of DMT Modulation

DMT is a multicarrier modulation technique where a high-speed serial data stream is divided into multiple parallel lower-speed streams and modulated onto multiple subcarriers of different frequencies for simultaneous transmission [6], [7].

Based on the fast Fourier transform (FFT) algorithm, multicarrier modulation and demodulation are efficiently implemented with DMT. Contrary to OFDM [18], the DMT modulator output signal after the inverse FFT ($IFFT$) is real-valued and no in-phase and quadrature (IQ-) modulation onto a radio frequency (RF) carrier is required [6], [8].

Therefore, broadband, high-frequency, analog RF-components required for IQ-modulation are omitted from DMT transceivers, reducing system costs and complexity. As a result, only a single digital-to-analog (D/A) converter and a single analog-to-digital (A/D) converter is needed to respectively generate and capture a DMT sequence.

A common misconception of DMT is that it requires twice as much hardware complexity when compared to OFDM. This, however, is not true. A possible reason that gives rise to such a misconception is that in order to generate a multicarrier sequence consisting of N subcarriers, DMT requires the use of an $IFFT$ operation which is twice the length of the one needed for OFDM. Similar, of course, applies to the case of demodulation with an FFT.

As will be shown in (2.1), real-valued input and output sequences of respectively an FFT and $IFFT$ are characterized by symmetry properties. As a result, the operations can be optimized for DMT modulation and half of the number of computations can be saved.

Therefore, DMT and OFDM require approximately the same amount of complexity and the longer $IFFT$ / FFT lengths needed for DMT are not disadvantageous.

In Fig. 2.1, the principle of DMT is shown.

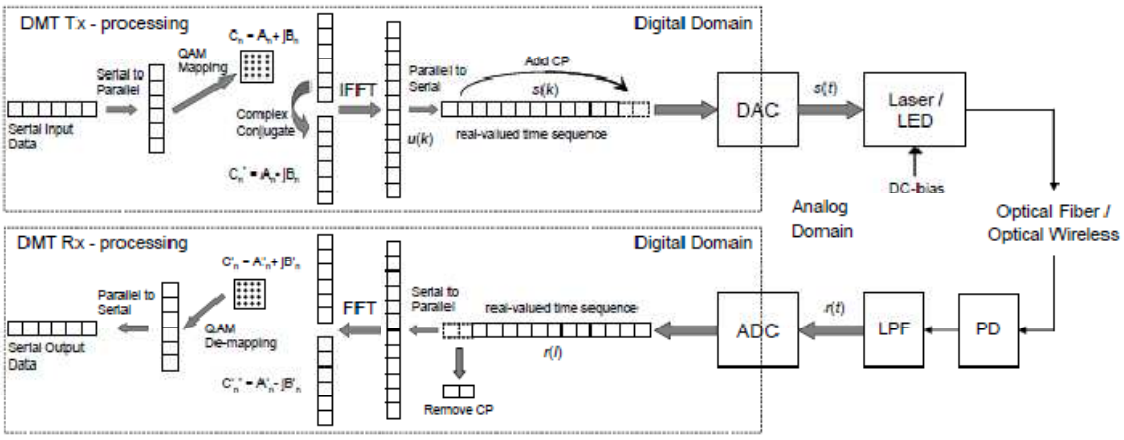

Figure 2.1 Schematic block diagram showing the principle of DMT over an optical IM/DD channel. DAC: digital-to-analog converter, ADC: analog-to-digital converter, LED: light-emitting diode, PD: photodetector, LPF: low-pass anti-aliasing fiilter, CP: cyclic prefix.

A high-speed binary serial input data sequence is divided into N parallel lower-speed binary streams. For each stream indexed by n, where $n = 0, 1, 2 \dots N-1$, every M number of bits are grouped together and mapped onto complex values $C_n = A_n + jB_n$ according to a quadrature amplitude modulation (QAM) constellation mapping consisting of 2^Mstates. Usually, the $IFFT$ is used in the DMT transmitter to efficiently modulate the complex values C_n onto N different subcarrier frequencies, which, as a result, are mutually orthogonal.

In order to achieve a real-valued, baseband DMT transmission sequence consisting of N subcarriers, a $2N$ -point $IFFT$ is needed. For the $2N$ inputs of the $IFFT$, indexed by $n = 0, 1 \dots 2N-1$, to the first half are assigned the values C_n and to the second half have to be assigned the complex conjugate values of C_n, following the Hermitian symmetry property given by

$$C_{2N-n} = C_n^* \tag{2.1}$$

for $n = 0, 1, 2 \dots N-1$ and $Im\{C_0\} = Im\{C_N\} = 0$. The $Im\{\ \}$ operator denotes the imaginary part. In practice, it is common to set $C_0 = C_N = 0$ so that the resulting DMT sequence does not contain any direct current (DC) value at all.

Following this, the output $u(k)$ of the $2N$-point $IFFT$ is always real-valued which can be proven by,

$$\begin{aligned} u(k) &= \frac{1}{\sqrt{2N}} \sum_{n=0}^{2N-1} C_n \, exp\left(j2\pi n \frac{k}{2N}\right) \\ &= \frac{1}{\sqrt{2N}} \sum_{n=0}^{N-1} \left\{ C_n exp\left[j2\pi n \frac{k}{2N}\right] + C_n^* exp\left[j2\pi (2N-n) \frac{k}{2N}\right] \right\} \\ &= \frac{1}{\sqrt{2N}} \sum_{n=0}^{N-1} \left\{ C_n exp\left[j2\pi n \frac{k}{2N}\right] + \left[C_n \exp\left(j2\pi n \frac{k}{2N}\right)\right]^* \right\} \\ &= \frac{1}{\sqrt{2N}} \sum_{n=0}^{N-1} 2 \cdot Re\left\{ C_n exp\left[j2\pi n \frac{k}{2N}\right] \right\} \end{aligned} \tag{2.2}$$

$$for\ k = 0, 1, 2, \ldots 2N - 1$$

Additionally, notice from Fig. 2.1 that a cyclic prefix (CP) is added to $u(k)$ before D/A conversion. The CP is a copy of the last fraction of $u(k)$, which is inserted in front of $u(k)$. For a CP with a length of NCP, the overall sequence can be represented as

$$s(k) = \frac{1}{\sqrt{2N}} \sum_{n=0}^{2N-1} C_n \exp\left(j2\pi n \frac{(k - N_{CP})}{2N}\right)$$

$$\text{for } 0 \leq k \leq 2N - 1 + N_{CP} \quad (2.3)$$

This $(2N + N_{CP})$-point sequence $s(k)$corresponds to the samples of the multicarrier DMT time-discrete sequence to be transmitted, which is here referred to as a DMT frame. Taking the sampling speed of the D/A converter into account, (3.4) is written as

$$s(k) = \frac{1}{\sqrt{2N}} \sum_{n=0}^{2N-1} C_n \exp\left(j2\pi n \frac{(k - N_{CP})\Delta t_s}{T}\right)$$

$$\text{for } 0 \leq k \leq 2N - 1 + N_{CP} \quad (2.4)$$

where $\Delta t_s = 1/f_s$ depicts the sampling period of the D/A converter and f_s its sampling frequency. T is the period of a DMT frame, defined as

$$T = (2N + N_{CP}) \cdot \Delta t_s \quad (2.5)$$

where $1/T = f_{sc}$ is also known as the subcarrier frequency spacing.

Note that this subcarrier frequency spacing f_{sc} is not a system parameter that can be chosen freely, but results indirectly from N, N_{CP} and the D/A converter sampling speed f_s.

Depending on the D/A converter impulse response $h_{DAC}(t)$, the resulting time continuous waveform of each DMT frame after D/A conversion can be written as

$$s(t) = \sum_{k=0}^{2N-1+N_{CP}} s(k)\, \delta(t - k\Delta t_s) \otimes h_{DAC}(t) \quad (2.6)$$

where ⊗ denotes the linear convolution operator and $\delta(t)$ the Dirac impulse. Due to the sample-and-hold function of most D/A converters, $h_{DAC}(t)$ can be modeled as a rectangular pulse ranging from 0 to Δt_s.

Assuming transmission over a linear and lossless channel, the (noise-free) received DMT frame $r(t)$ at the receiver (directly before A/D conversion) can be characterized as

$$r(t) = \sum_{k=0}^{2N-1+N_{CP}} s(k)\,\delta(t-k\Delta t_s) \otimes h(t) = \sum_{k=0}^{2N-1+N_{CP}} s(k)\,p(t-k\Delta t_s) \qquad (2.7)$$

where $p(t)$ is the pulse shaping function given by

$$p(t) = \delta(t) \otimes h(t) = \int_{-\infty}^{\infty} \delta(\tau) h(t-\tau)\,d\tau \qquad (2.8)$$

and $h_{DAC}(t) \otimes h_{ch}(t) \otimes h_f(t)$ is the combined impulse response of the D/A converter $h_{DAC}(t)$, the entire channel including the electrical-to-optical and optical-to-electrical conversion $h_{ch}(t)$, and the low-pass, anti-aliasing filter response $h_f(t)$ before A/D conversion.

In order for the DMT frames to be received and demodulated properly, two conditions have to be satisfied:

1. The length of the DMT frame without CP, given by $T - N_{CP} \cdot \Delta t_s$should be longer than or at least equal to the time length of $h(t)$ in order to avoid inter-frame interference.

2. N_{CP} should be chosen so that its time period $N_{CP} \cdot \Delta t_s$ is longer or equal to the time length of $h(t)$.

Assuming ideal sampling instances and no sampling frequency offset, every received DMT frame $r(t)$ is sampled by the A/D converter with a sampling speed of $f_s = 1/\Delta t_s$, resulting in the discrete samples

$$r(l\Delta t_s) = \sum_{k=0}^{2N-1+N_{CP}} s(k)\,p(l\Delta t_s - k\Delta t_s) = \sum_{k=0}^{2N-1+N_{CP}} s(k)\,p[(l-k)\Delta t_s] \qquad (2.9)$$

where, ideally, l should consist of integer values given by $l = -\infty, \ldots, \infty$. However, efficient demodulation of a DMT frame is accomplished by use of

a 2N-point FFT, so that $r(l\Delta t_s)$ can only consist of $2N$-points per DMT frame. If N_{CP} is chosen so that its time period $N_{CP} \cdot \Delta t_s$ is long enough to represent the entire pulse shape $p(t)$, choosing $l = N_{CP}, N_{CP}+1, \dots, 2N-1+N_{CP}$ will result in FFT demodulation of a DMT frame $r(l\Delta t_s)$ given by

$$\begin{aligned}
\hat{C}_n &= \sum_{l=N_{CP}}^{2N-1+N_{CP}} r(l\Delta t_s) \exp\left[-j2\pi(l-N_{CP})\frac{n}{2N}\right] \\
&= \sum_{l=N_{CP}}^{2N-1+N_{CP}} \sum_{k=0}^{N_{CP}} s(k)\, p[(l-k)\Delta t_s] exp\left[-j2\pi(l-N_{CP})\frac{n}{2N}\right] \\
&= H_n \cdot \sum_{l=N_{CP}}^{2N-1+N_{CP}} s(l) exp\left[-j2\pi(l-N_{CP})\frac{n}{2N}\right] \\
&= H_n \cdot \sum_{k=0}^{2N-1} u(k) exp\left(-j2\pi k\frac{n}{2N}\right) \\
&= |H_n| \cdot \exp(-j\phi_n) \cdot C_n \qquad (2.10)
\end{aligned}$$

H_n is the $2N$-point FFT of the channel impulse response $h(t)$ at index/subcarrier n, where $n = 0, 1, \dots, 2N-1$. This can also be considered as a multiplicative gain $|H_n|$ and a phase shift $(-j\phi_n)$ of each subcarrier in the received DMT frame.

Usually, preamble DMT frames with known data values are transmitted in a DMT system in order to estimate $|H_n|$ and $(-j\phi_n)$ of the transmission channel. At the receiver, multiplying $\hat{C}_n$ with $1/H_n$ will result in the transmitted symbols C_n. This operation is often denoted as one-tap, zero-forcing, frequency-domain equalization.

From (2.10), it can be seen that inclusion of the CP allows the linear convolution of the DMT frame $s(t)$ with the channel impulse response $h(t)$ to be converted into a cyclic convolution. Therefore, demodulation with the FFT will result in just a complex multiplication of the sent data symbols with the channel response. When no CP is used, demodulation with the FFT will result in inter-carrier interference.

Naturally, the inclusion of a CP comes at the expense of additional redundancy.

2.2 DMT in an Optical IM/DD Channel

Especially in low-cost optical communication systems such as multimode fiber and optical wireless systems, intensity-modulation and direct-detection (IM/DD) is employed where only the intensity of light is modulated and not the phase. Such systems do not need such high levels of performance like long-haul single-mode fiber systems because of the much shorter reach. Moreover, due to its enormous market volume and low sharing factor, it is essential that the cost level of short-range optical communication systems is lowered to the bare minimum. It is therefore most straightforward and easy to modulate the intensity of an optical source such as an LED or a laser diode just by modulating its driving current. Consequently, at the receiver side, only the intensity of the received optical signal needs to be detected. A simple photodiode is enough to detect this intensity, making an IM/DD optical communication system the cheapest system for transmitting information by optical means.

Next to the principle of DMT, Fig. 2.2 also shows how DMT can be applied in an optical IM/DD channel. Such an application of DMT is different from standard electrical systems, where a bipolar baseband signal is used. However, the intensity of the optical source can only have positive values. In IM/DD DMT systems, this problem is commonly solved by adding a DC-bias to the bipolar DMT signal to make it unipolar [3]. This is also shown in Fig. 2.1, where a DC-bias is added to the electrical (AC-coupled) DMT waveform before driving the laser or light-emitting diode of a short-range optical communication system. At the receiver, a simple (lowcost) photodetector is used to detect the intensity of the received light. This converts the DMT signal, which was modulated on the intensity, to an

electrical signal which is then sampled by an analog-to-digital A/D converter for further digital processing.

Other techniques for DMT over IM/DD channels exist, without the need to add a DC-bias to the DMT signal. One such example is asymmetrically-clipped optical OFDM (ACO-OFDM), where the bipolar DMT waveform is clipped at the zero value and only the positive parts are transmitted [3].

2.2.1 The IM/DD Channel Model

Fig. 2.2 shows a block diagram of a intensity modulated direct detection (IM/DD) optical communication system. The data is modulated onto an electrical signal, $s(t)$. Depending on the details of the electrical system, $s(t)$ may be represented by either current or voltage; however in either case the electrical power is proportional to $s^2(t)$. The optical intensity modulator generates an optical signal with intensity (not amplitude) $s(t)$. This means that $s(t)$ can take only positive values and so modulation techniques commonly used in radio communications cannot be used without modification. The signal is passed through an optical channel with impulse response, $h(t)$. The signal $r(t)= h(t) \otimes s(t)$ is received by a direct detection receiver which converts the optical intensity signal back to an electrical signal (voltage or current), $Rr(t)$.

The system model shows AWGN being added in the electrical domain. This is the model commonly used in wireless infrared communication systems [19] where the main impairment is due to high level ambient infrared radiation. The ambient signals are mainly at DC and can be filtered out, however they cause shot noise in the detector, which is accurately modeled as AWGN. The received noisy signal is

$$z(t) = Rr(t) + w(t)$$

where $w(t)$ is AWGN. The data is recovered from $z(t)$ using a matched filter. The BER of the system depends on $z(t) = s(t) + w(t)$

In many optical communication systems, the average transmitted optical power, given by,

$$E\{s(t)\} = \lim_{T\to\infty} \frac{1}{2T} \int_{-T}^{T} s(t)dt \qquad (2.11)$$

is constrained by eye safety considerations. This means that while the main constraint on signal design is the value of $E\{s(t)\}$, the BER depends on the electrical SNR which depends on $E\{s^2(t)\}$. Therefore the performance of a system depends not only on the type of modulation (orthogonal, bipolar etc.) but on the average optical power. In contrast to radio systems where a high peak-to-average ratio is a disadvantage, in optical systems signals with a high peak-to-average ratio in general give better system performance as the ratio $E\{s^2(t)\}$ to $E\{s(t)\}$ is large and so they have a larger received electrical power for a given optical power [19].

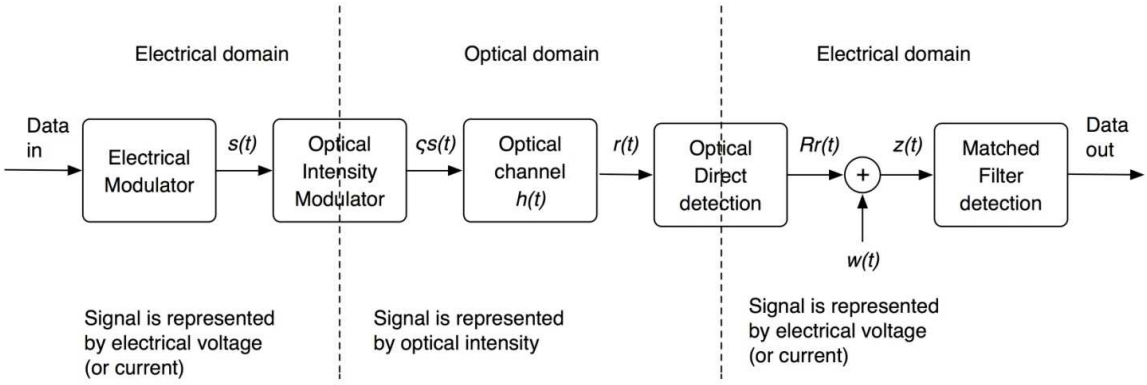

Fig 2.2 Block diagram of a intensity modulated direct detection optical communication system

2.2.2 DC-Biased

The main method of DMT over optical IM/DD channels is the one with DC-bias, as depicted in Fig. 2.1. In [25] this technique is also denoted as adaptively-modulated optical OFDM (AMOOFDM).

AMOOFDM is generated by introducing OFDM into the optical domain, and subsequently by manipulating the modulation format of individual

subcarriers within an AMOOFDM symbol according to the frequency response of a given transmission link.

Apart from the fastest ever capacity-versus-reach performance, the AMOOFDM technique also reveals the following unique characteristics [25].

1) Significant flexibility and robustness: through negotiations between the transmitter and the receiver in the initial stage of establishing a transmission link, optimized transmission performance is always achievable regardless of link specification, transmission distance, and signal capacity. This feature may lead to a solution that "one box" fits all applications.

2) Efficient use of spectral characteristics of transmission links: AMOOFDM is capable of exploiting the link bandwidth to its full potential. This technique has a spectral efficiency that significantly exceeds limits associated with all traditional signal modulations and digital signal processing.

3) Cost effective in system installation and maintenance; in addition, the cost of an AMOOFDM modem is also significantly low. It is estimated that the cost of such a modem would be about 25% of a commercially available optical modem designed for 10-Gb/s metro transmission systems.

The general modeling procedures of the AMOOFDM modems can be described as follows: in the transmitter, an incoming binary data sequence is encoded to serial complex numbers by using different signal-modulation formats. A serial-to- parallel converter truncates the encoded complex data sequence into a large number of sets of closely and equally spaced narrowband data, the so-called subcarriers, and each set contains the same number of subcarriers. An inverse fast Fourier transform ($IFFT$) is then applied to each set of subcarriers to generate parallel real-valued AMOOFDM symbols. These AMOOFDM symbols are serialized to form a

long digital signal sequence, to which signal clipping is applied for the purpose of limiting the AMOOFDM signal power within a predetermined range. Finally, a digital-to-analog converter (DAC) is used to convert the digital data sequence into an analog signal waveform, which is ready to drive directly a laser to produce an optical AMOOFDM signal waveform at 1550 nm.

In the receiver, the optical signal emerging from the link is detected by a square-law photodetector. After passing through a low-bandpass filter and an analog-to-digital converter (ADC), the electrical signal is decoded into the original sequence by the receiver, which is the inverse of the transmitter described above.

For the generation of a real-valued AMOOFDM signal waveform, the encoder in the transmitter is modified to create AMOOFDM symbols with the original data in the positive frequency bins and the complex conjugate of the data in the negative frequency bins. The bipolar signal is converted to a unipolar signal by adding a DC bias.

Generally speaking, a high (low) modulation format is used on a subcarrier suffering a low (high) transmission loss. The total channel bit error rate (BER) BER_T is defined as

$$BER_T = \frac{1}{N_s - 1} \sum_{K=0}^{N_s-1} BER_k \qquad (2.12)$$

where BER_k is the signal BER corresponding to the k-th subcarrier. N_s is the total number of subcarriers within an AMOOFDM symbol. A high modulation format is always preferred if BER_T remains at 1.0×10^{-3} or better, which leads to an error-free operation when combined with forward error correction (FEC). On the other hand, subcarriers suffering very high losses may be dropped if the BER_k corresponding to each of those carriers is still unacceptable even when DBPSK is used.

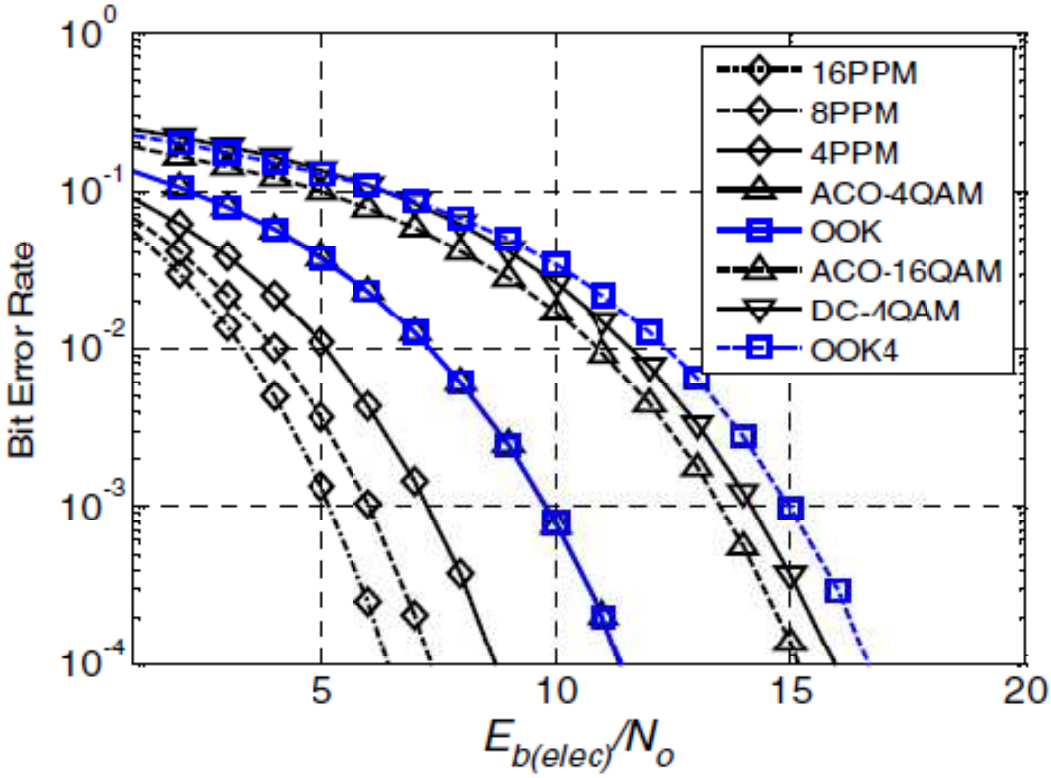

Figure 2.3 BER as a function of $E_{b(elect)}/N_0$ for PPM, OOK, ACO-OFDM and DC biased OFDM [12]

2.2.3 ACO

In the papers that describe the use of OFDM in IM optical communications, a large DC bias is usually added to the OFDM signals but this results in an optical signal with a high mean optical power [26]. This is very inefficient and makes conventional OFDM impractical in the many optical systems in which the average transmitted optical power is limited due to eye safety or other considerations.

Recent work by the authors has shown that by asymmetrically clipping particular classes of bipolar OFDM signals, power efficient Optical OFDM signals can be derived [2], [9]. ACO-OFDM signals retain the properties that make OFDM resilient in a dispersive or multipath channel.

[12] show that for a given average transmitted optical power and signal bandwidth ACO-OFDM gives better performance than PPM and OOK (see Fig 2.3). This result has significant practical implications for both wireless optical and optical fiber communications. In many optical systems the

achievable data rate is limited by a combination of maximum transmitted optical power and multipath distortion, ACO-OFDM solves the multipath problem as well as giving a 2 dB reduction in optical power for an AWGN channel.

Principles of ACO-OFDM

Fig. 2.4 shows samples of a typical OFDM baseband symbol and the waveform $x(t)$ which could be generated from them. Fig. 2.5 shows a symbol where only odd subcarriers are used. OFDM signals have a high peak-to-average power ratio. For $N \geq 64$ the central limit theorem applies and the distributions of $x(k)$ and $x(t)$ are approximately Gaussian.

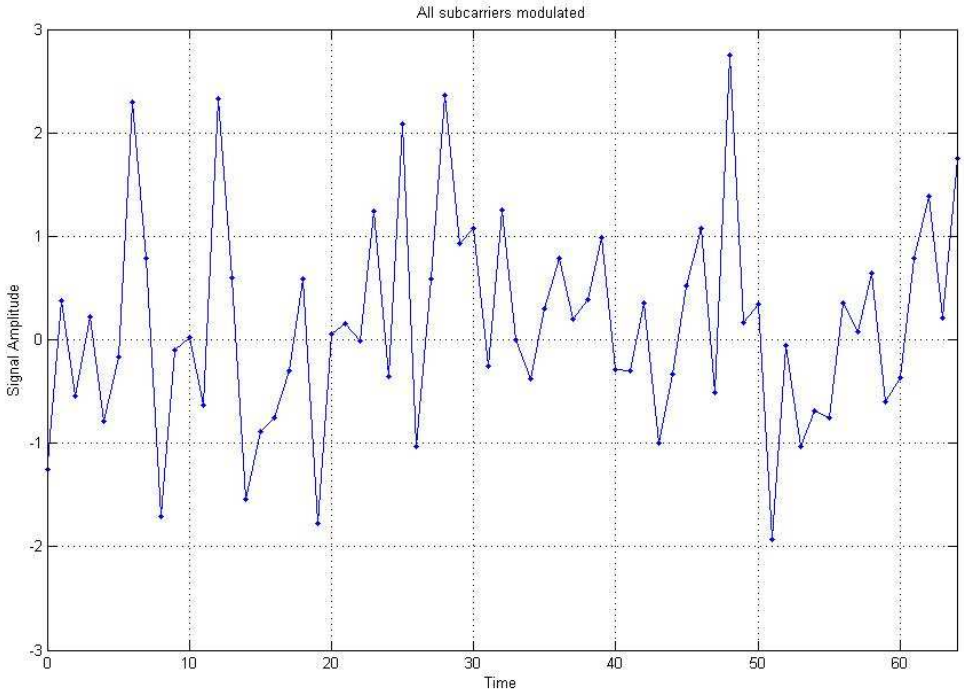

Fig 2.4 An OFDM symbol consisting of all the subcarriers

In the ACO scheme the signal $x_c(k)$ shown in Fig. 2.6b would be transmitted. All negative values are forced to zero. It will show that if the subcarrier frequencies used for data transmission are correctly chosen, the data can be retrieved from a signal of this form with little, or for some configurations, no in-band clipping noise.

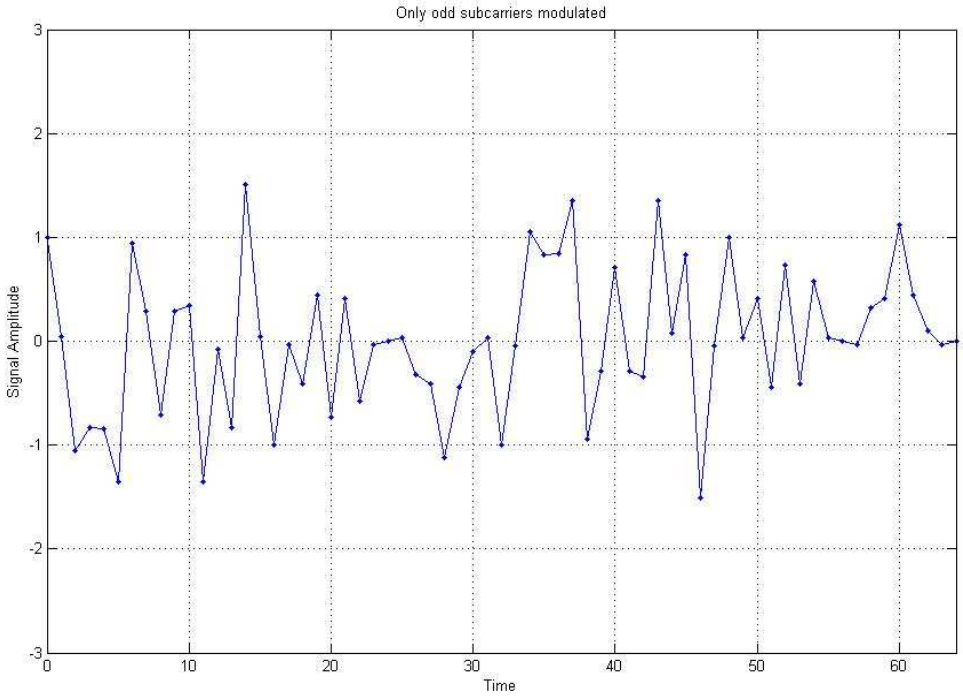

Fig 2.5 An OFDM symbol consisting of only odd frequencies

Analysis of clipping

Clipping is a memoryless nonlinear operation on $x(k)$. As $x(k)$ has a Gaussian distribution, Bussgang's theorem can be applied [2]. Thus

$$x_c(k) = Kx(k) + d(k) \qquad (2.13)$$

where K is a constant and $d(k)$ is a random noise process which is uncorrelated with $x(k)$ so $E[d^*(k)x(k)] = 0$. Thus multiplying (2.13) by $x^*(k)$ and taking the expectation $E[.]$ gives

$$K = \frac{E[x_c(k)x^*(k)]}{E[x(k)x^*(k)]} \qquad (2.14)$$

$x(k)$ is real so $x^*(k) = x(k)$. Also as $x(k)$ is symmetrically distributed about zero

$E[x_c(k)x(k)] = E[x(k)x(k)]/2$ and therefore $K = 1/2$ and $x_c(k) = x(k)/2 + d(k)$. Thus clipping the signal at zero reduces the amplitude of the wanted signal by half, but advantageously it reduces the mean optical power,

$E[x_c(k)]$, by much more. $x_c(k)$ is zero with probability 0.5 and has a semi-normal distribution otherwise, so

$$E[x_c(k)] = \left(1/\sqrt{2\pi}\right) \int_0^\infty z\, exp(-z^2/2) dz = 1/\sqrt{2\pi} \qquad (2.15)$$

Thus the average optical power of $x_c(k)$ is approximately $1/\sqrt{2\pi}$ compared to 2 for DC-biased optical OFDM. The amplitude of each OFDM subcarrier is also reduced by a factor of 0.5. When both the electrical and optical effects of clipping are considered, the electrical amplitude of each subcarrier is increased by a factor of 0.5 x 2 x $\sqrt{2\pi}$ compared with DC-biased OFDM with the same average optical power.

Thus the overall improvement in electrical signal-to-noise ratio is $20 \log_{10}\left(\sqrt{2\pi}\right) = 7.98\, dB$.

Clipping also adds an unwanted noise component, $d(k)$. Most of the noise power is in the $zero$-th subcarrier and is easily separated from the OFDM signal, but some is at other frequencies.

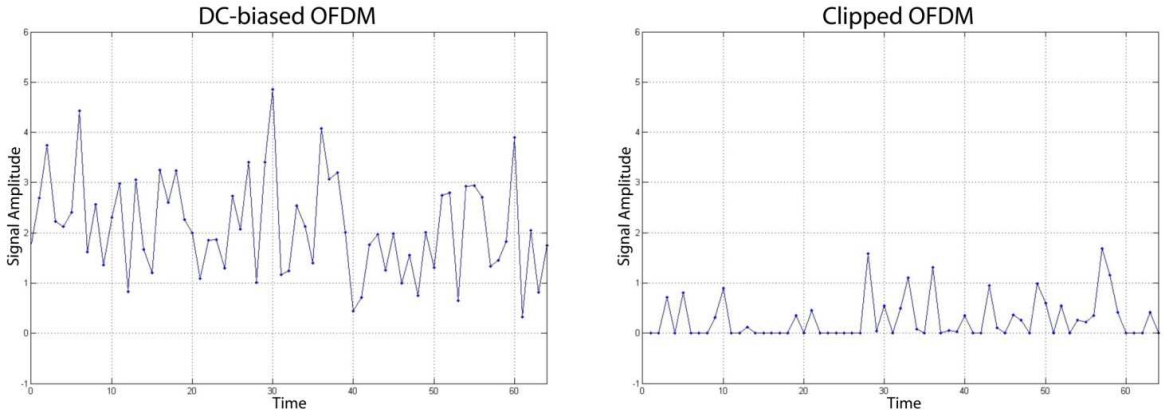

(a)

(b)

Fig 2.6 An OFDM symbol consisting of only odd frequencies

Frequency distribution of clipping noise

The distribution of the energy of $d(k)$ across subcarrier frequencies depends on which subcarriers are used in the unclipped OFDM signal. If

only the odd subcarriers of $x(k)$ in a symbol are nonzero then it can be shown that $d(k)$ has components at even frequencies only. Consider the properties of the $IFFT$ and FFT and the relationship between $x(k)$ and $x(k+N/2)$ for odd subcarriers only. The component of $x(k)$ due to the m-th subcarrier is given by

$$x(m,k) = (1/N)X(m)\exp\left(\frac{j2\pi km}{N}\right) \tag{2.16}$$

Thus, it is simple to show that for m odd $x(m,k) = -x(m,k+N/2)$. Thus an OFDM symbol consisting of only odd frequencies has the property that $x(k) = -x(k+N/2)$ as shown in Fig. 2.5. The value of $X(m)$ can be calculated from $x(k)$ using an FFT,

$$X(m) = \sum_{k=0}^{N-1} x(k)exp\left(\frac{-j2\pi km}{N}\right) \tag{2.17}$$

To derive the properties of the clipped signal it is useful to modify (2.17) to give

$$\begin{aligned} X(m) = \frac{1}{N}\sum_{\substack{k=0 \\ x(k)>0}}^{N/2-2} x(k)\,exp\left(\frac{-j2\pi km}{N}\right) \\ +x\left(k+\frac{N}{2}\right)exp\left(\frac{-j2\pi(k+N/2)m}{N}\right) \\ +\frac{1}{N}\sum_{\substack{k=0 \\ x(k)<0}}^{N/2-2} x(k)\exp\left(\frac{-j2\pi km}{N}\right) \\ +x\left(k+\frac{N}{2}\right)exp\left(\frac{-j2\pi(k+N/2)m}{N}\right) \end{aligned} \tag{2.18}$$

If only odd subcarriers are nonzero then the second term in each of the summations in (2.18) is equal to the first term so

$$X(m) = \frac{2}{N} \sum_{\substack{k=0 \\ x(k)>0}}^{N/2-2} x(k)\, exp\left(\frac{-j2\pi km}{N}\right) + \frac{2}{N} \sum_{\substack{k=0 \\ x(k)<0}}^{N/2-2} x(k)\, exp\left(\frac{-j2\pi km}{N}\right) \qquad (2.19)$$

Now consider the case of clipping a signal with only odd frequencies. Then in (2.18) only the first term in the first summation and the second term in the second summation are nonzero. Thus comparing with (2.18) and summing over the positive signal values gives

$$X_c(m) = \frac{1}{N} \sum_{k=0}^{N-1} x_c(k)\, exp\left(\frac{-j2\pi km}{N}\right) = \frac{X(m)}{2} \qquad (2.20)$$

Thus clipping in this case results in the amplitude of each of the (odd) data carrying subcarriers being exactly half of their original value and therefore all of the clipping noise must fall on the even subcarriers. Thus the received signal can be demodulated in exactly the same way as a standard OFDM system, the data is recovered from the odd subcarriers and the even subcarriers are discarded.

This analytical result was confirmed by simulation. Fig. 2.7 shows the scatter plot for 4-QAM and $N = 32$ with only odd subcarriers carrying data. The constellation points before clipping were $\{\pm 1, \pm j\}$. After clipping the constellation points for the odd subcarriers become as predicted $\{\pm 0.5, \pm 0.5j\}$ and the even subcarriers have a noise-like distribution.

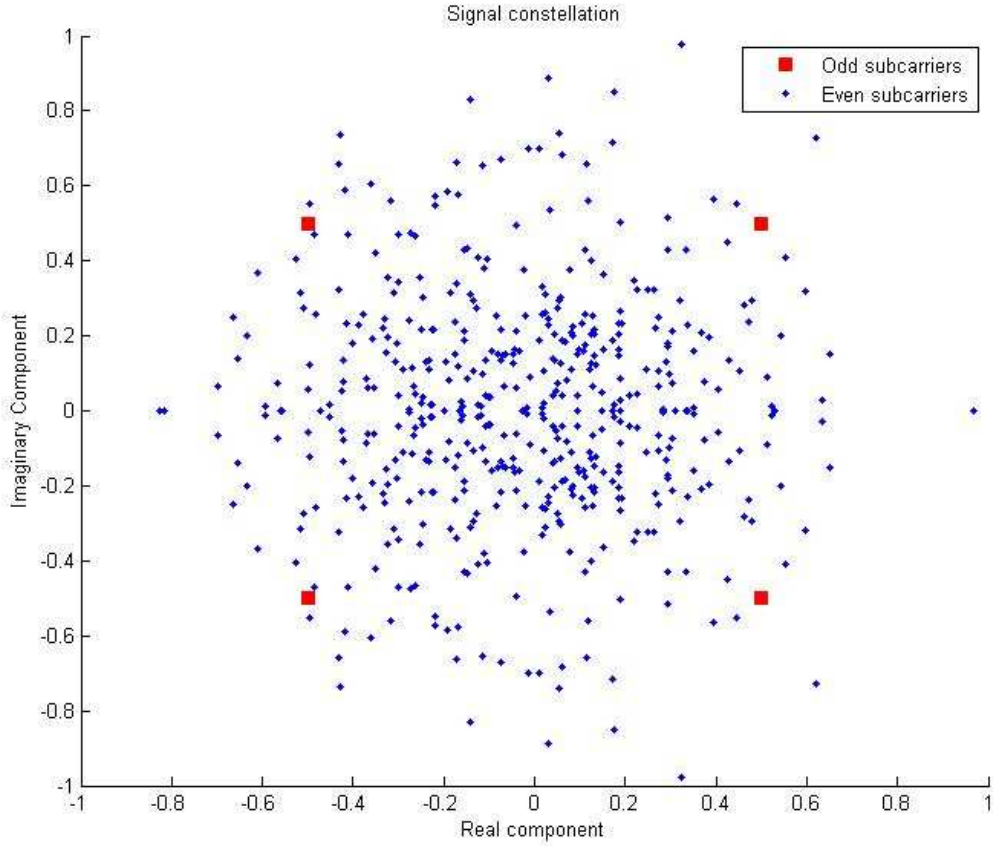

Fig 2.7 Constellation after clipping

2.2.4 Comparison between DCO-OFDM and ACO-OFDM

In DCO-OFDM the bipolar OFDM signal is converted to a unipolar signal by adding a DC bias, B_{DC}. In practice because an OFDM signal has a Gaussian distribution, if B_{DC} is not to be excessive, the peaks of the negative going signal must first be clipped. This adds a clipping noise component, $n_C(B_{DC})$, which increases as B_{DC} decreases and affects all subcarriers.

$$x(t) = x_0(t) + B_{DC} + n_C(B_{DC}) \approx x_0(t) + B_{DC} \qquad (2.21)$$

The optimum clipping level depends on the signal constellation. For practical BERs, large constellations such as 256-QAM require very high SNRs, so clipping noise must be very low and therefore B_{DC} must be large. This also increases the optical power because, $Popt = E\{x\} \approx B_{DC}$. Unlike ACO-OFDM where the same configuration is optimum for all constellations,

when DCO-OFDM is combined with adaptive modulation and different constellations are used on different subcarriers, B_{DC} cannot be optimized for all constellation sizes. The Hermitian constraint means that for DCO-OFDM there are $N/2$ independent complex inputs for an N point $IFFT$, so for a given constellation size the data rate of DCO-OFDM is twice that of ACO-OFDM.

Fig. 2.8 shows the BER of DCO-OFDM for 4, 16, 64 and 256-QAM and for B_{DC} set relative to the power of $x_0(t)$,

$$B_{DC} = k\sqrt{E\{x_0^2(t)\}} \qquad (2.22)$$

The literature define this as a bias of $10\log_{10}(k^2 + 1)$ dB, as this is the increase in the power of the DCO-OFDM signal relative to $x_0(t)$. To demonstrate the effect of a moderate and large bias, values of 7 dB and 13 dB are used. Increasing the bias has two effects: it increases the electrical power and it reduces the clipping noise. For high levels of bias the clipping noise is negligible and the required $E_{b(elec)}/N_0$ for a given BER is approximately equal to the $E_{b(elec)}/N_0$ for a bipolar signal plus the bias level (in dB). For larger constellations and lower levels of AWGN, the clipping noise dominates and the BER graphs plateau.

In ACO-OFDM the bipolar OFDM signal generated by the transmitter $IFFT$ is made unipolar by clipping the signal at zero

$$x(t) = \begin{cases} x_0(t) \;\; if \;\; x_0(t) \geq 0 \\ 0 \;\; if \;\; x_0(t) \leq 0 \end{cases} \qquad (2.23)$$

where $x_0(t)$ is the unclipped OFDM signal [2]. It was already shown that if only the odd frequency subcarriers are modulated all of the intermodulation caused by clipping falls on the even subcarriers and does not affect the data-carrying odd subcarriers [2]. The odd frequency and Hermitian constraint together mean that there are only $N/4$ independent complex input values for an N point IFFT.

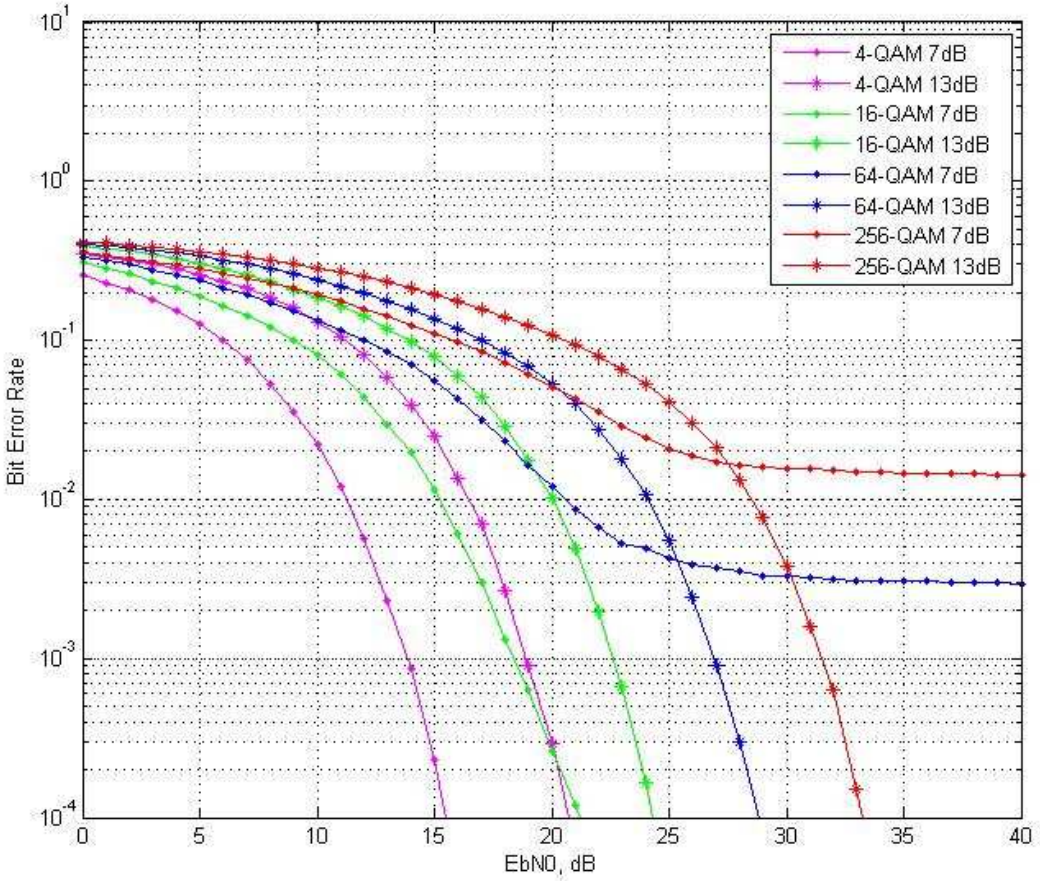

Fig 2.8 BER of DCO-OFDM for 4, 16, 64 and 256-QAM

Fig. 2.9 shows simulation results for the BER of ACO-OFDM as a function $E_{b(elec)}/N_0$ for different QAM constellations and an additive white Gaussian noise (AWGN) channel. This model is commonly used in optical wireless systems where the noise is bipolar (not unipolar) because the main noise source is in the electrical front-end of the receiver.

4-QAM ACO-OFDM requires 3 dB more power than bipolar 4 QAM. This has a simple theoretical explanation [3]: in ACO-OFDM only half of the electrical power is used on the odd frequency, data-carrying subcarriers. The other half is used on the even subcarriers to make the ACO-OFDM signal unipolar [2]. This is also true for all constellation sizes so ACO-OFDM always requires 3 dB more power than a bipolar system using the same constellation.

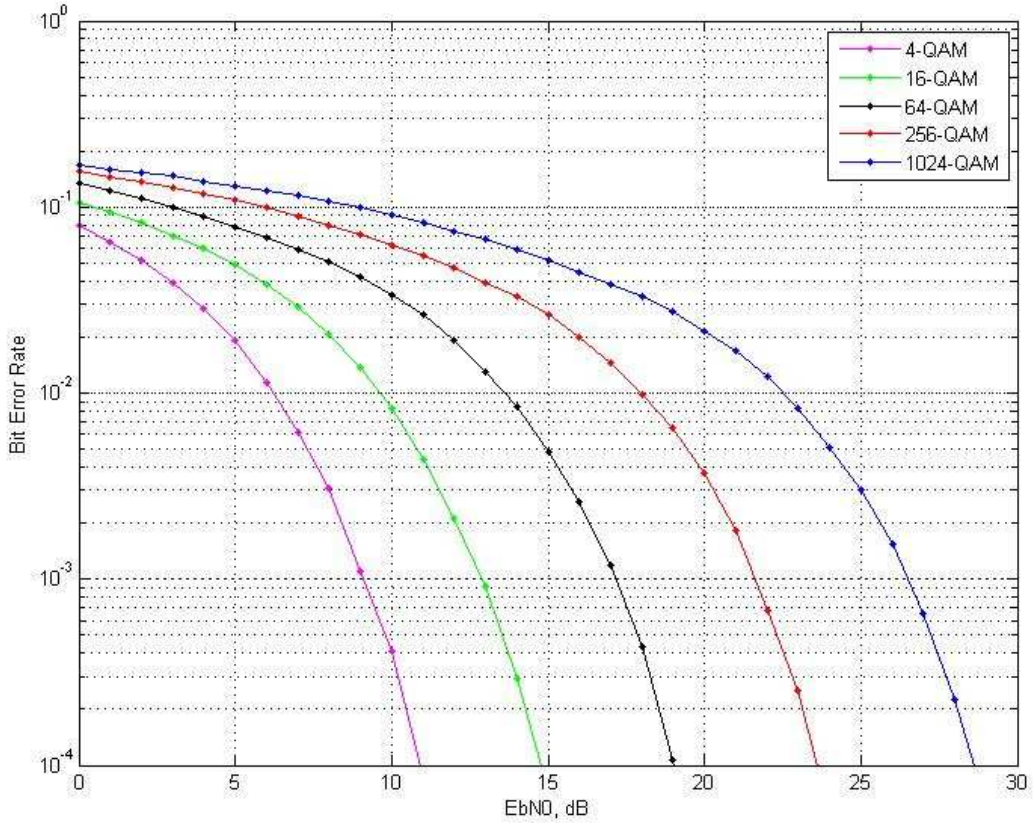

Fig 2.9 BER of DCO-OFDM for 4, 16, 64 and 256 and 1024-QAM

Thus, for a given normalized bandwidth ACO-OFDM requires less power than DCO-OFDM for all but the largest constellations. The performance of DCO-OFDM depends on the bias. A large bias increases the required power, while a low bias results in clipping noise which limits performance. For ACO-OFDM the same design is optimum for all constellation sizes, making ACO-OFDM better suited to adaptive systems.

CHAPTER 3
Optical OFDM based on Discrete Hartley Transform

An alternative optical OFDM scheme can be based on a real trigonometric transform to directly deal with real signal. In [27] is proposed a novel optical OFDM scheme based on the discrete Hartley transform (DHT) for power efficient transmission in IM/DD systems.

The discrete Hartley transform (DHT) resembles the discrete Fourier transform (DFT) but is free from two characteristics of the DFT that are sometimes computationally undesirable:

- the inverse DHT is identical with the direct transform, and so it is not necessary to keep track of the $+i$ and $-i$ versions as with the DFT.
- the DHT has real rather than complex values and thus does not require provision for complex arithmetic or separately managed storage for real and imaginary parts.

Nevertheless, the DFT is directly obtainable from the DHT by a simple additive operation. DHT permits faster computing. Since the speed of the fast Fourier transform depends on the number of multiplications, and since one complex multiplication equals four real multiplications, a fast

Hartley transform also promises to speed up Fourier-transform calculations.

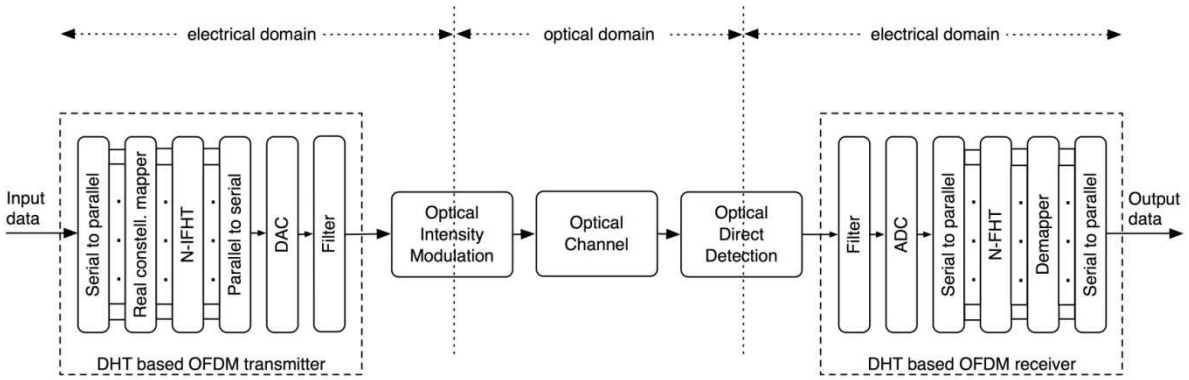

Fig. 3.1 Block diagram of an IM/DD system, using optical OFDM based on Harley Transform. The input is mapped into a real constellation of OFDM modulated by the N-order IFHT. The demodulation uses the direct FHT.

3.1 DHT

Hartley transform is particularly attractive for the processing of real signals. The direct and inverse transforms are identical, and the Hartley transform of a real signal is real. Fourier transform always implies a complex processing and the phase carries fundamental information, while Hartley transform is a real trigonometric transform. Furthermore, the real and imaginary parts of the discrete Fourier transform (DFT) coincide with the even and the negative odd parts of the DHT, respectively: the transform kernels only differ for the imaginary unit [28]. DFT is used to perform the OFDM modulation, because it can be seen as a bank of modulators, whose narrowband channels have mutually orthogonal subcarriers. Similarly, the mirror-symmetric sub-bands of DHT ensure subcarriers orthogonality, and the spectral behavior enable to carry the data symbols for the parallel processing.

Therefore, fast Hartley transform (FHT) can replace FFT algorithm to furnish an alternative OFDM scheme. If the input symbols are real, the inverse FHT (IFHT) gives real OFDM signals. When the OFDM signals are real valued, the multicarrier transmission technique is considered a special

case of OFDM: no in-phase and quadrature modulation onto an RF carrier is required and in the literature it is referred as discrete multi-tone modulation (DMT) [5], [8]. Because of the DHT real processing, a simpler transmission system can be achieved. In [27], the DHT-based solution proposed in [29] is adapted to optical systems.

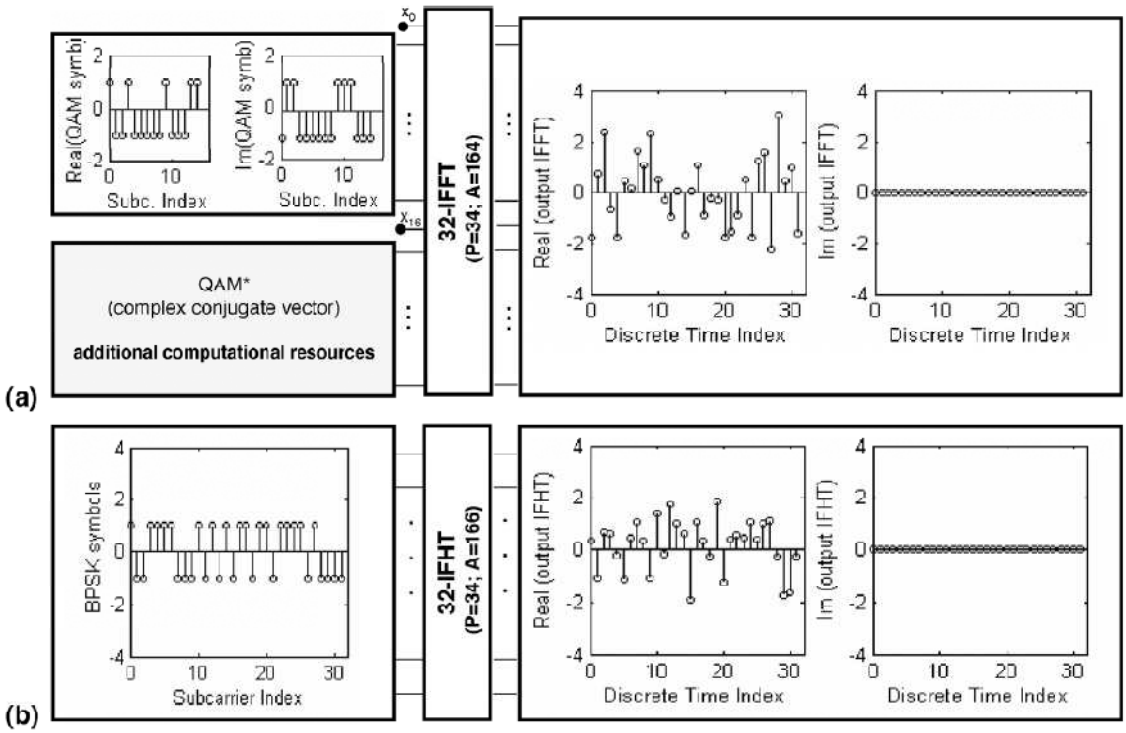

Fig. 3.2 (a)Real-valued discrete outputs of a 32-order IFFT. The input sequence has Hermitian symmetry, and it is given by the half-length vector of 4 QAM symbols and the corresponding complex conjugate vector. The dc and Nyquist frequencies are set to zero. (b) Real-valued discrete DHT-based OFDM symbol, evaluated as the 32-order IFHT of a BPSK vector of length 32. The number of multiplications (P) are additions (A) reported un the figure have been evaluated according to the FFT and FHT algorithms with the minimum arithmetic complexity.

3.2 OPTICAL OFDM SYSTEM BASED ON DHT

The block diagram of the DHT-based optical OFDM system is depicted in Fig. 3.1. The $IFHT$ and FHT are used in place of the inverse FFT ($IFFT$) and FFT, to perform the OFDM modulation and demodulation, respectively. According to the definition of DHT [28], the OFDM symbol is given by

$$h(k) = \frac{1}{\sqrt{N}} \sum_{n=0}^{N-1} x(n) \left[cos\left(\frac{2\pi kn}{N}\right) + sin\left(\frac{2\pi kn}{N}\right) \right] \qquad (3.1)$$

$$for\ k = 1, 2, \dots, N-1$$

Where $x(n)$ indicates the symbol sequence and N represents the number of symbols processed in parallel. The DHT kernel is real, and it can also be indicated as [28]

$$cas\left(\frac{2\pi kn}{N}\right) = cos\left(\frac{2\pi kn}{N}\right) + sin\left(\frac{2\pi kn}{N}\right) \qquad (3.2)$$

If a real constellation [e.g., binary phase-shift keying (BPSK), *M*-PAM (pulse-amplitude modulation)] is used for the subcarriers modulation, the OFDM symbol $h(k)$ is real. If the input symbols are complex, $h(k)$ is complex.

In order to obtain real-valued IFFT, the input vector must have Hermitian symmetry. Fig. 3.2(a) shows the real-valued OFDM symbol at the output of a 32-order IFFT. The information sequence is mapped into 4 QAM symbols; the second-half of the input vector is given by their complex conjugate values [indicated in Fig. 3.2(a) as QAM]. The dc and Nyquist frequencies that are $x(0)$ and $x(N/2)$, respectively, are set to zero. For a given OFDM signal bandwidth, when the number of subcarriers is doubled the carrier spacing decreases accordingly.

On the other hand, for a given bit rate, by maintaining the same carrier spacing, if only half of the available subcarriers are used to carry data, the required bandwidth to transmit the same data signal increases accordingly. For a given constellation size, the data rate that can be supported by the double of subcarriers is greater. In DMT systems, only half of the IFFT points are used to process the information data symbols (independent complex values); the second-half is required to process the complex conjugate vector, due to the Hermitian symmetry constrain [8]. When DHT is used, Hermitian symmetry is not required: if the input vector is real, the IFHT is real-valued and the number of subcarriers carrying

information symbols (independent real-valued values) coincides with the DHT points, as shown in Fig. 3.2(b). So that to transmit the same data signal, a lower constellation size (BPSK) is required.

As shown in Fig. 3.1, by using the DHT, the input data stream is serial-to-parallel converted and mapped into a real constellation to generate a real OFDM signal. After parallel-to-serial conversion, the real OFDM signal can be processed by one single digital- to-analog converter (DAC). The analog signal is real, but it is still bipolar and must be converted into unipolar to be IM. As it will be demonstrated, both AC and DC-biased solutions, adopted in standard optical OFDM, are possible for DHT-based optical OFDM.

Adding a DC-bias requires more power and residual clipping noise can affect the transmission.

By adopting AC technique the average optical power is reduced without affecting the transmission.

At the receiver, after DD, the signal is converted to digital by one single analog-to-digital converter (ADC) and the sequence is recovered by DHT processing and demodulating the signal.

As in the standard implementation of OFDM, a cyclic prefix (CP) can be used to mitigate intersymbol interference and intercarrier interference [29]. The choice of prefix length should take into account that this overhead reduces the supported data rate, to cope with the delay introduced by the channel. Generally, the CP is a small fraction of the OFDM symbol, but to be effective should be longer than the delay spread.

Due to the double-side band optical spectrum, ACO-OFDM does not enable to compensate for significant fiber chromatic dispersion [27]. In fact, the intensity modulation generates an OFDM signal on both sides of the optical carrier frequency. DD is more robust to dispersion impairments when combined with optical single-side band modulation than when direct IM is applied [30].

3.3 Asymmetrically Clipped DHT-Based O-OFDM

With a suitable choice of the subcarriers to be modulated, the DHT-based OFDM signal can be clipped at zero level and correctly recovered without clipping noise.

In fact, as for DFT, also for DHT it is easy to demonstrate that for n odd

$$h\left(n, k+\frac{N}{2}\right) = -h(n,k) \tag{3.3}$$

Therefore, if only the odd subcarriers are nonzero, the DHT-OFDM symbol is obtained by clipping the IDHT evaluated for a BPSK sequence of length N. The sequence $x(n)$ can be recovered by simply performing the Hartley transform of the IDHT-OFDM symbol

$$x(n) = \frac{1}{\sqrt{N}} \sum_{k=0}^{N-1} h(k) \left[cos\left(\frac{2\pi kn}{N}\right) + sin\left(\frac{2\pi kn}{N}\right)\right] \tag{3.4}$$

By making explicit the symbol elements in the summation, it can be rewritten in the following form

$$x(n) = \frac{1}{\sqrt{N}} \sum_{k=0}^{N/2-1} h(k)\, cas\left(\frac{2\pi kn}{N}\right) + h\left(k+\frac{N}{2}\right) cas\left(\frac{2\pi kn}{N} + \pi n\right) \tag{3.5}$$

Stated (3.3) and according to the assumption that only the odd subcarriers are nonzero

$$x(n) = \frac{2}{\sqrt{N}} \sum_{\substack{k=0 \\ h(k)<0}}^{N/2-1} h(k)\, cas\left(\frac{2\pi kn}{N}\right) + \frac{2}{\sqrt{N}} \sum_{\substack{k=0 \\ h(k)>0}}^{N/2-1} h(k)\, cas\left(\frac{2\pi kn}{N}\right) \tag{3.6}$$

where the summation in (3.5) has been split in two, depending on the sign of $h(k)$. For clipped signal $h_c(k)$

$$h_c(k) = \begin{cases} h(k) & h(k) \geq 0 \\ 0 & h(k) < 0 \end{cases} \tag{3.7}$$

only one of the two terms of (3.5) is nonzero, depending on the sign of $h(k)$; therefore, the recovered symbol sequence will be

$$r(n) = \frac{1}{\sqrt{N}} \sum_{k=0}^{N-1} h_c(k)\, cas\left(\frac{2\pi kn}{N}\right) = \frac{x(n)}{2} \qquad (3.8)$$

This means that, as in ACO-OFDM based on FFT [2], the symbol sequence can be recovered from the odd subcarriers, and the constellation points have the half of the original values. All the clipping noise falls into the even subcarriers that can be easily discarded. As clipping is a memoryless nonlinearity, the attenuation of the input sequence and the presence of additive noise directly follow the Bussgang's theorem. It can be applied because $h(k)$ can be assumed to have a Gaussian distribution for $N \geq 64$. Therefore, the same analysis of clipping reported in [2] can be considered valid also for the DHT-OFDM signal.

3.4 Performance Analysis

This section analyze the performance of the proposed IM/DD optical OFDM communication systems based on DHT, in an AWGN channel, adding a Gaussian noise source in the electrical domain, after DD, in the system represented in Fig. 3.1. In order to compare the performance of the proposed system, with ACO and DC-biased O-OFDM systems based on FFT presented by other authors [12], [3], and analyzed in chapter 2, the same assumptions will be considered. The comparison proposed is between DMT systems based on N-order DHT, and DFT able to transmit the same data signal per OFDM symbol. The impulse response of the optical channel is considered unitary, and no CP will be considered. For the analysis of DC-biased solution, will be evaluated the performance for bias values of 7 and 13 dB, assuming the same bias definition of the chapter 2:

$$B_{DC} = k\sqrt{E\{x_0^2(t)\}} \qquad (3.9)$$

and considering its value in dB as $10\log_{10}(k^2 + 1)$; $E\{x_0^2(t)\}$ is the signal variance.

Fig. 3.4 reports the bit error rate (BER) as a function of the bit electrical energy normalized to the noise power spectral density $E_{b(elec)}/N_0$.

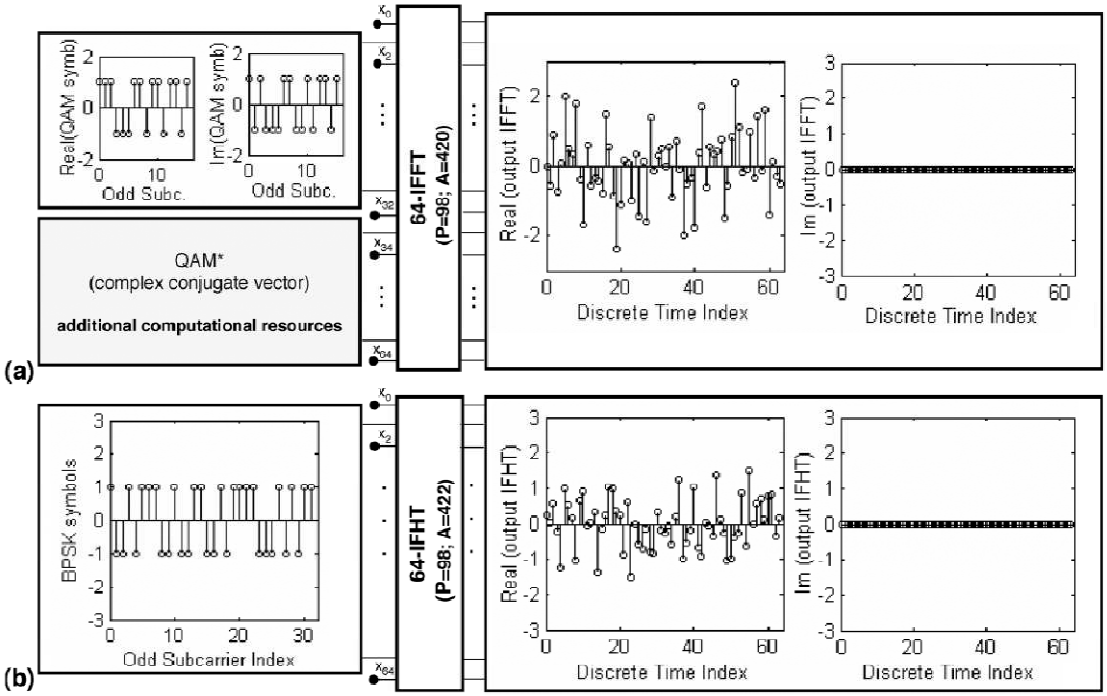

Fig. 3.3 16 symbols 4 QAM and 32 symbols BPSK representing the same input sequence of 32 bits and the corresponding real-valued discrete OFDM symbols using (a) a 64-order IFFT, (b) a 64-order IFHT

The power efficiency of AC technique is superior to DC-biased solution also for optical DHT-based OFDM, as shown in Fig. 3.4. The DHT has the same performance of the DMT case. However, due to the AC, which reduces the recovered symbols to half of the original values, in ACO-OFDM 3 dB more power is required compared to a bipolar system, using the same constellation [3]. Only half of the power is used for the odd subcarriers, the rest is converted into clipping noise carried by the even subcarriers. In the case of DC-biased O-OFDM, all the subcarriers are used to modulate the input symbols, while in the case of AC, only the odd subcarriers are used for modulation.

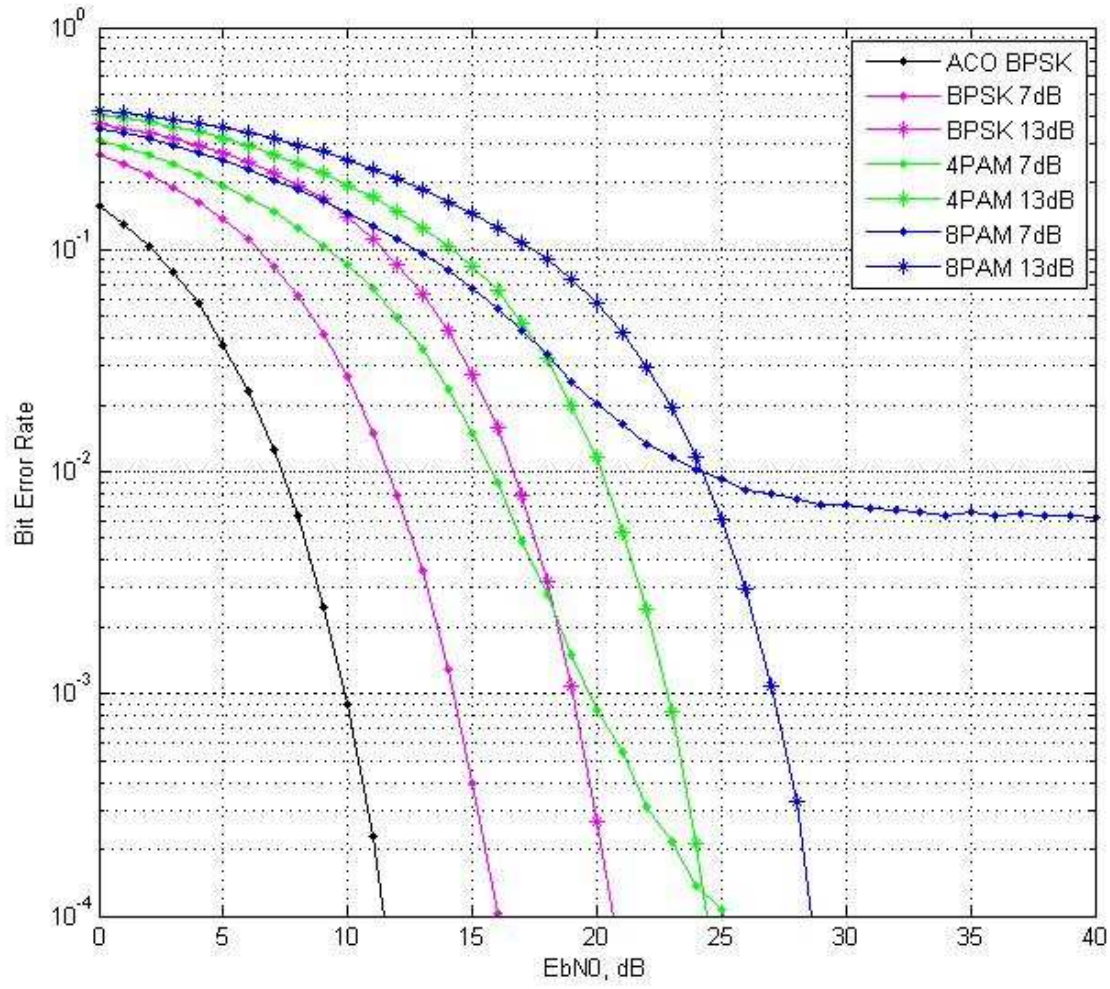

Fig 3.4 BER versus normalized bit electrical energy (Eb $E_{b(elec)}/N_0$) for BPSK ACO and DC-biased OFDM based on DHT in AWGN channel.

There is a tradeoff between bandwidth efficiency and power efficiency. In fact, Fig. 3.5 shows that to obtain a BER of 10^{-3}, DC-biased OFDM with a bias of two times the standard deviation requires a normalized bit energy value about 4 dB greater than the $E_{b(elec)}/N_0$ of ACO-OFDM. In this performance evaluation, were take into account the additional noise due to the clipping at zero level of DC-biased signal. If the bias value is larger, the additional noise due to the clipping of residual negative peaks decreases. This is at expenses of the electrical power, as it can be seen for the BER curve of Fig. 3.4, representing the performance of a DHT-based optical OFDM system using 13 dB as bias value.

Optical OFDM type	N-order DHT-based		N-order DFT-based	
	DC-biased	ACO	DC-biased	ACO
Supported constellation	Real (BPSK, M-PAM)		Complex (m-QAM)	
Constellation size	$M = 2^{\log_4 L}$		$m = L$	
Hermitian symmetry	NOT required		Required	
Computational complexity	$P = (N \log_2 N - 3N + 4)$ $A = (3N \log_2 N - 5N)/2 + 6$ Self-inverse NO add. resources		$P = (N \log_2 N - 3N + 4)/2$ $A = (3N \log_2 N - 5N)/2 + 4$ NOT self-inverse Resources for QAM*	
Subc. carrying info	N	N/2	N/2	N/4

Table 3.1 Comparison between DHT-based and DFT-based O-OFDM for IM/DD systems

As summarized in Table 3.1, the independent constellation symbols supported by an N-order FFT-based AC or DC-biased O-OFDM are $N/4$ and $N/2$, respectively. For DHT-based are $N/2$ and N, since the double of constellation symbols can be allocated. Therefore, in order to compare O-OFDM systems transmitting the same signal at the same bit rate, the input sequence of the DHT-based scheme is mapped into a real M-ary constellation that requires a lower value for M.

First comparison of the performance is on an AC DHT-based systems using a 2 levels modulation (BPSK) with the ACO-OFDM based on FFT analyzed in [12], where the modulation is a 4 QAM.

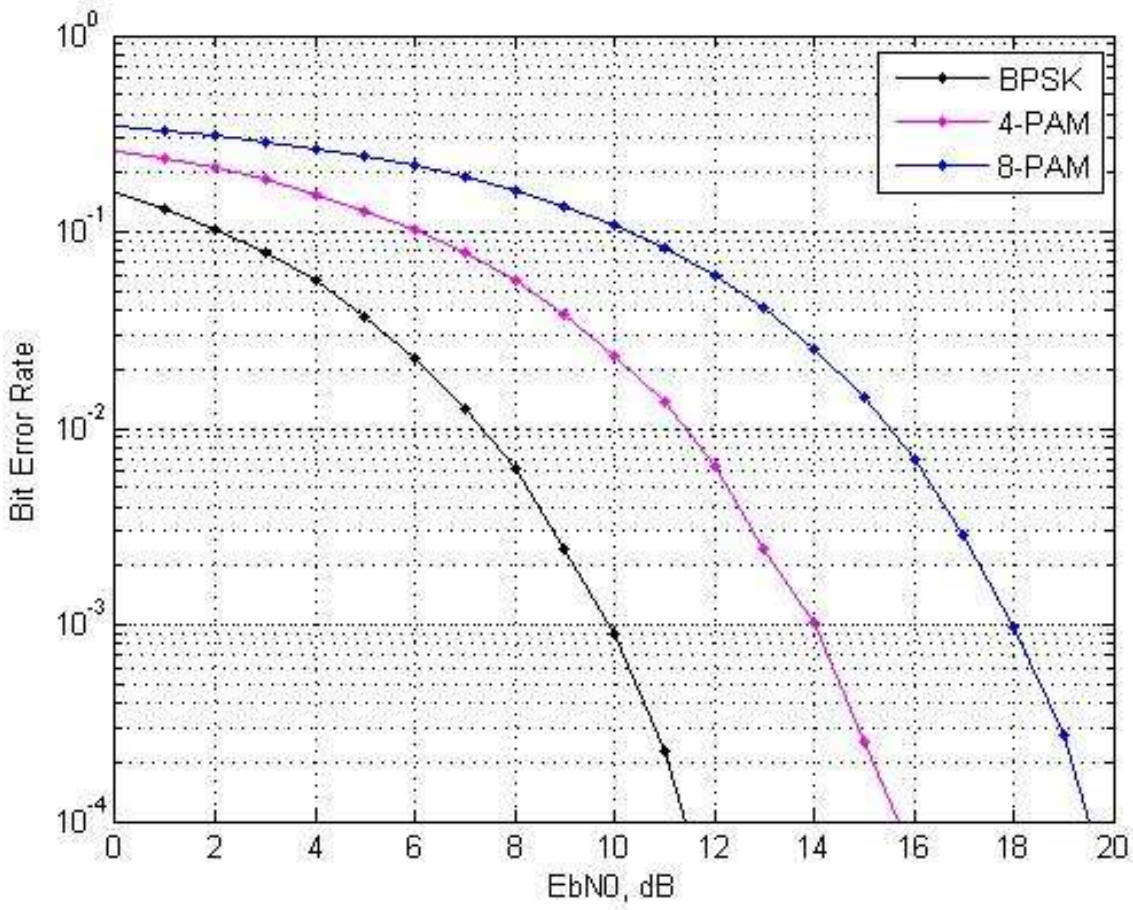

Fig. 3.5 BER versus normalized bit electrical energy (Eb $E_{b(elec)}/N_0$) for BPSK, 4 PAM, and 8 PAM ACO-OFDM based on DHT in AWGN channel.

It can be observed that the same performance can be achieved with a simpler scheme, using the DHT real processing. Similarly, the same BER curves can be obtained with a DC-biased DHT-based O-OFDM system, using BPSK or a 4 QAM DC-biased system based on FFT of the same order, transmitting the same data sequence. Again, let us compare the results with the curves in [3], observing good agreement. To benefit of the real processing offered by Hartley transform, only real constellation can be supported. The same data sequence at the same bit rate is transmitted with a simpler system, which does not require Hermitian symmetry for the input signal. In an IM/DD optical OFDM system, both FFT and FHT of the same order N can be used to transmit at the same bit rate. However, if L is the QAM constellation size, to achieve the same

performance, the size of the real constellation for the DHT is $M = 2^{\log_2(L)/2} = 2^{\log_4 L}$.

CHAPTER 4
Simulations

4.1 Simulation schemes

For all the simulations, VPIsystems' VPItransmissionMaker™ V8.5 was used.

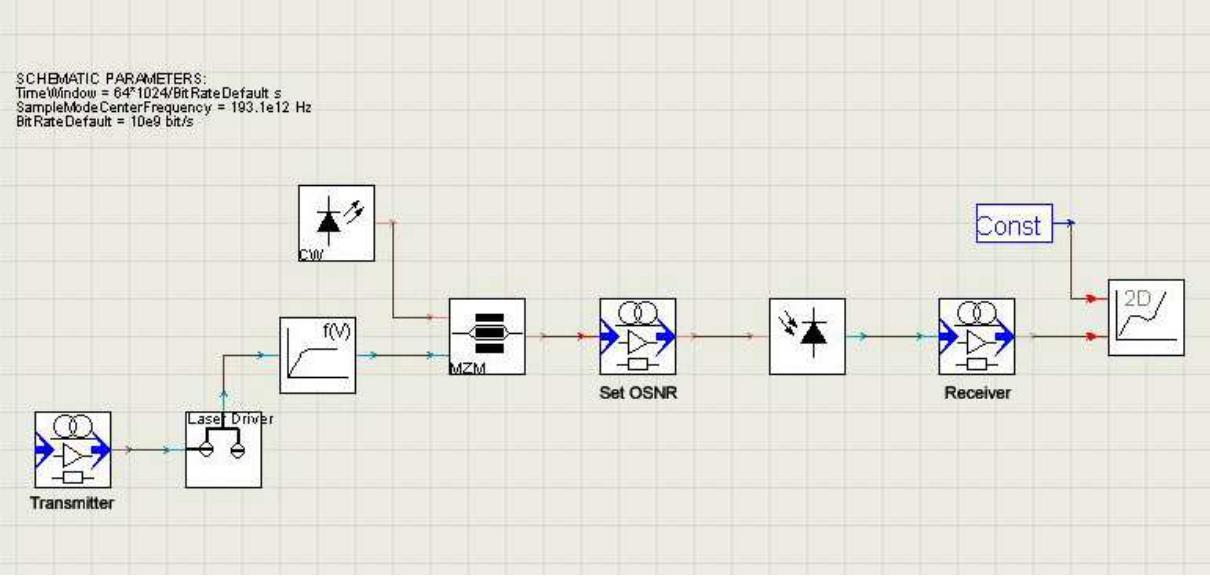

Fig 4.1 Transmission scheme

Figure 4.1 shows the transmission scheme used for simulations. After the transmitter, the electrical signal passes through a laser driver which

determines the bias and the amplitude of the electrical signal and, hence, through a limiter for clipping it at 0 to obtain a unipolar signal.

The laser has a center emission frequency of 193.1 THz and an average power of 0 dBm.

The modulator is a Mach-Zehnder, with Exinction 10 dB. The photodiode is APD, with responsitivity R = 0.7, avalanche x = 7. The thermal noise was set at 10 $pA / \sqrt{Hz}$.

Transmitter and receiver schemes are shown in Figure 2 and 3.

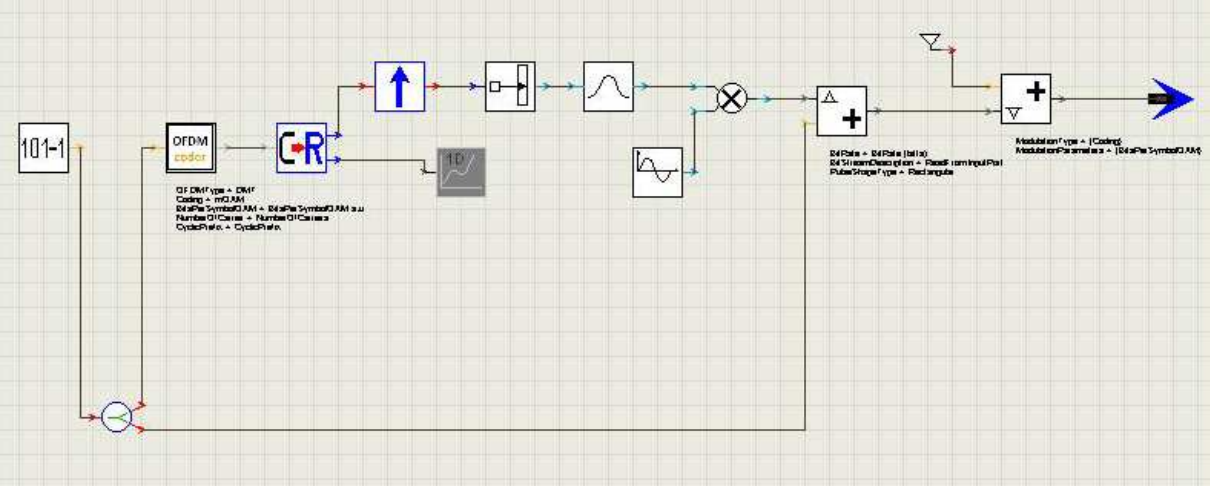

Fig. 4.2 Transmitter

In figure 4.2 is important to note that the OFDM coder has only one branch, corresponding to the real one. Has it was already shown in chapters 2 and 3, for the DMT case it is due to the Hermitian symmetry while in the DHT case, it is due to the real output of the Discrete Hartley Transform. To achieve a suitable comparison between the two transformations, the main modulation formats used are BPSK and 4-QAM: this, because in DMT systems, only half of the IFFT points are used to process the information data symbols, while the second-half is required to process the complex conjugate vector, due to the Hermitian symmetry constrain. On the other hand, when DHT is used, Hermitian symmetry is not required: if the input vector is real, the IFHT is real-valued and the number of subcarriers carrying information symbols coincides with the

DHT points. So that to transmit the same data signal, a lower constellation size (BPSK) is required for the DHT.

In [9], the autors showed that the maximum ($signal^2/variance$) under zero-bias clipping and obtained with high received powers depends on the RF sub-carrier frequency, f_{RF}, divided by the OFDM bandwidth, Δf_{OFDM}. The closer the lower-end OFDM band is to DC, the worse the noise due to clipping. This is because low-order intermodulation products due to clipping fall at difference frequencies between the OFDM carriers, and these are strongest near DC. Thus, the OFDM channels should be placed above the difference frequencies between the highest and lowest OFDM channels, and f_{RF} should be at least $1{,}5 \times \Delta f_{OFDM}$.

For this reason, the f_{RF} carriers was set to 15 GHz, to have a band of optical OFDM sub-carriers in the range 10-20 GHz above the optical carrier at 193.1 THz (See Figure 4.3).

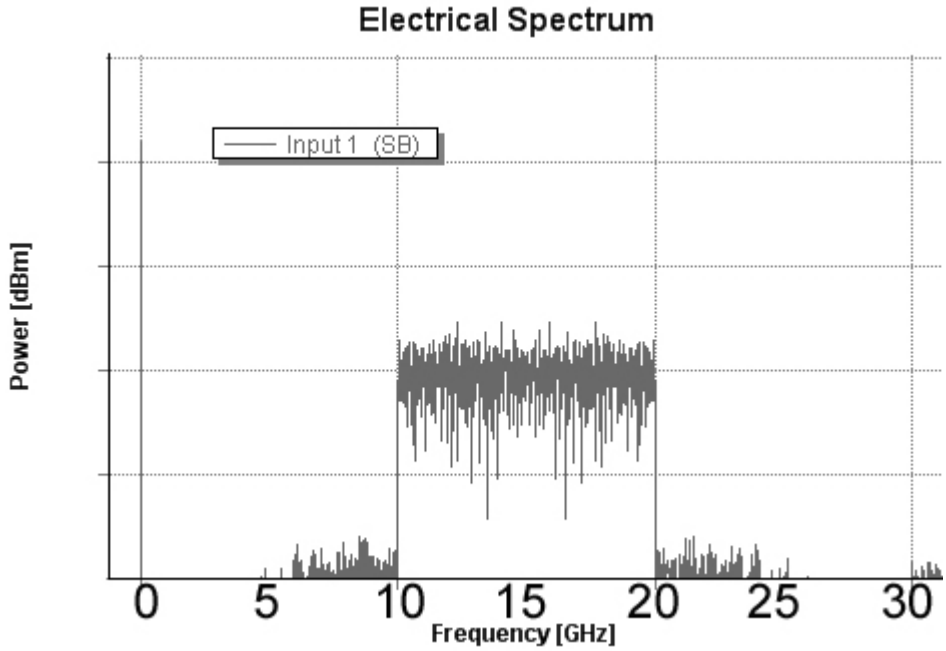

Fig. 4.3 Spectrum at the output of the photodiode

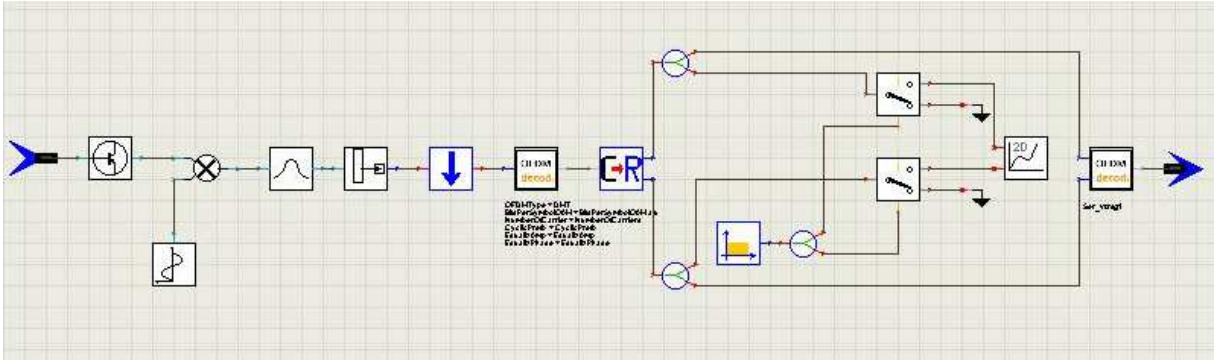

Fig. 4.4 Receiver

At the receiver the signal (still real) passes through an amplifier with gain G=0, a down-sampler and a OFDM decoder that realize the FFT (or DHT) of the signal. The last block realize the BER calculation and plot the received constellation.

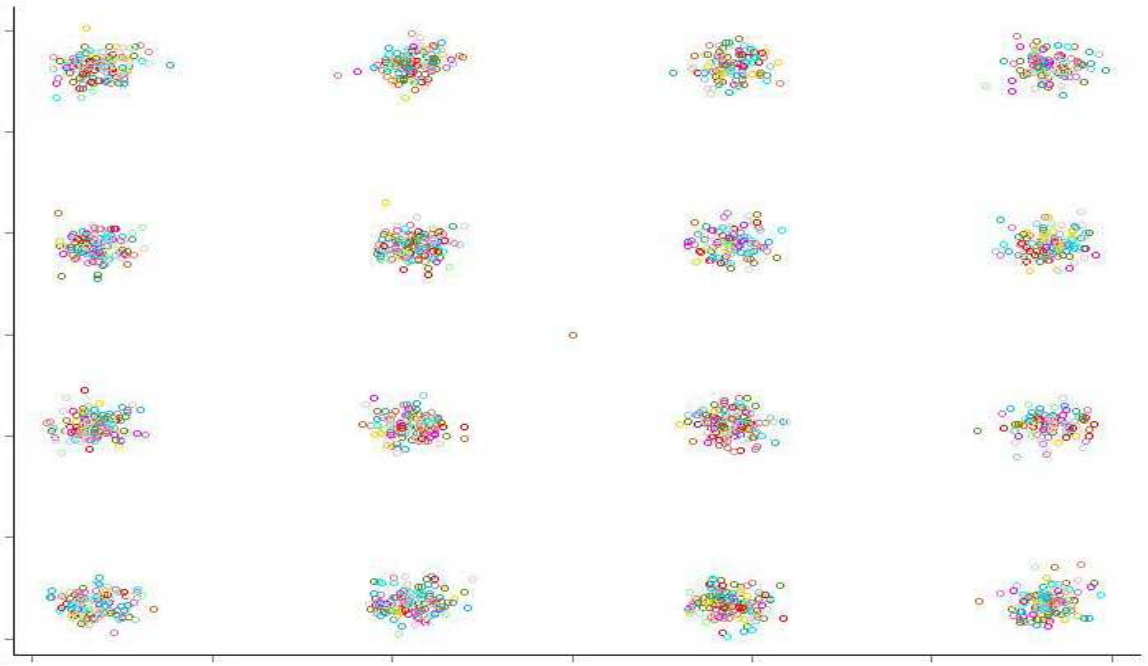

Fig. 4.5 Example of 16-QAM received constellation

4.2 Simulation results

4.2.1 DMT results

For the simulation of the DMT modulation scheme, the main difficulty encountered was the setting of the bias. During the simulation in Matlab described in Chapters 2 and 3, the bias was based on the standard deviation of the signal, consequently in dB: in the driver used in VPItransmissionMaker™ it was set as a voltage. Despite this differences, a reasonable result was achieve for values between 0.4 and 0.8 volts.

In this performance evaluation, were taken into account the additional noise due to the clipping at zero level of DC-biased signal. If the bias value is larger, the additional noise due to the clipping of residual negative peaks decreases.

The graph of figure 4.6 shows the behavior of the DMT scheme for a 4-QAM modulation: as expected, the curves tend to shift to the right with increasing bias. For a direct comparison see figure 2.8 of Chapter 2.

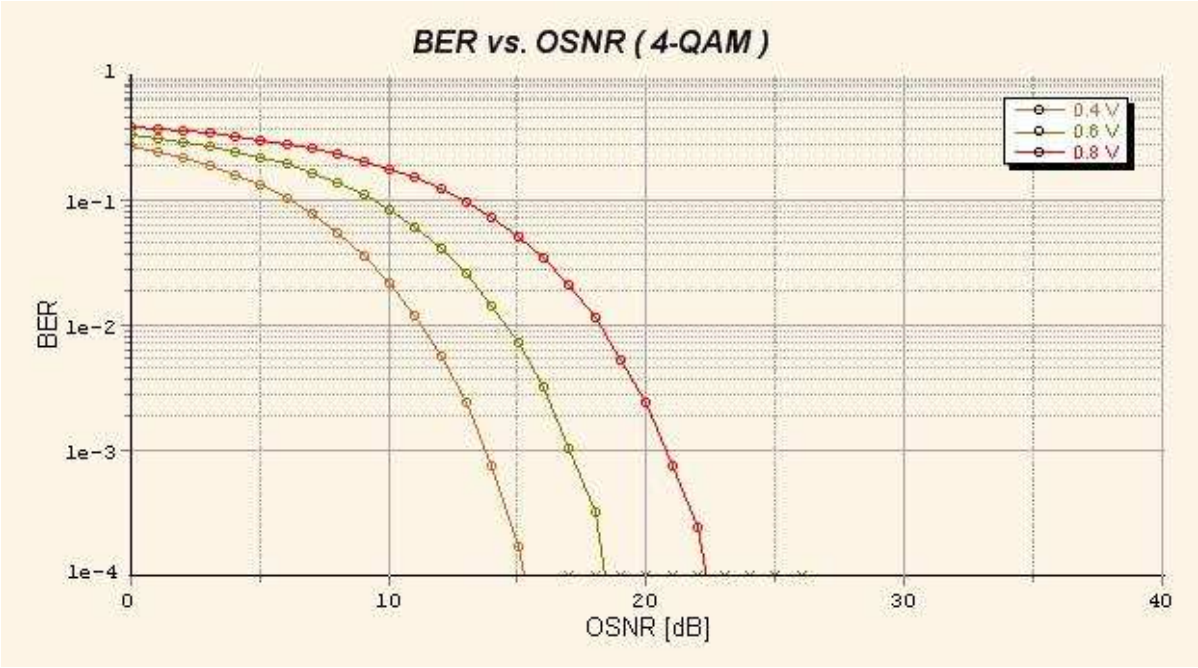

Fig 4.6 – BER as a function of OSNR for the DC-biased DMT and 4-QAM modulation for different bias

In figure 6 are shown the curves for a 16-QAM modulation. Also in this

case the graph is in line with the expected results: increasing the bits-per-symbol of the modulation degrades the performance.

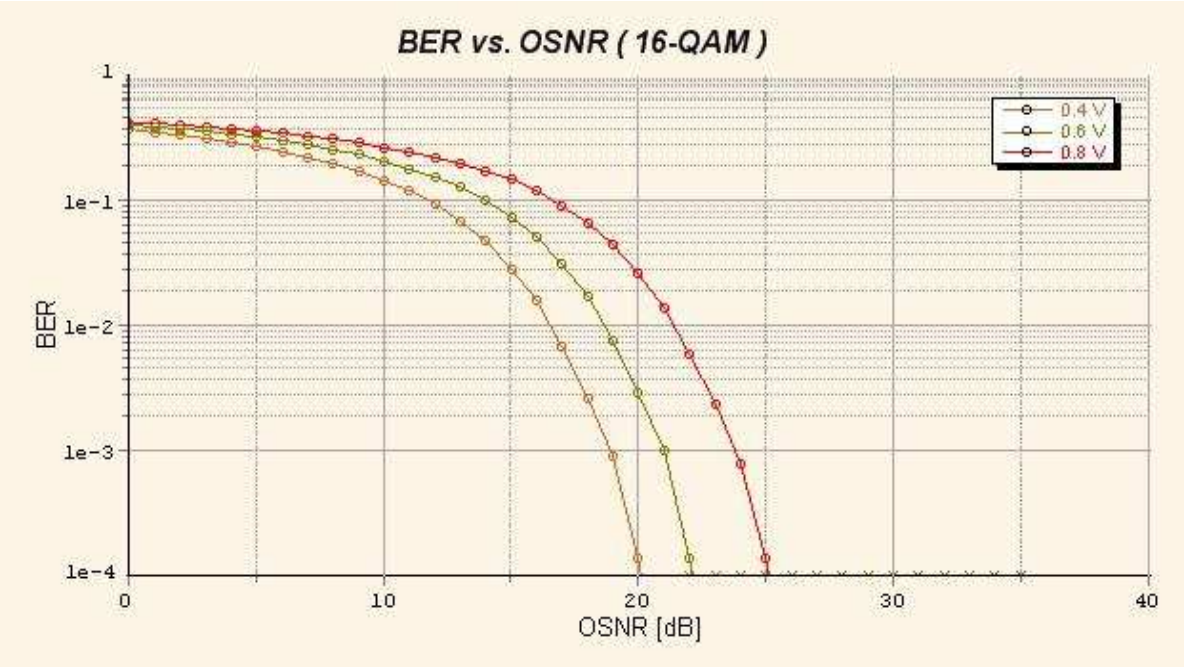

Fig 4.7 – BER as a function of OSNR for the DC-biased DMT and 16-QAM modulation for different bias

ACO-DMT

The principle of ACO-OFDM [2] [9], is to remove (clip) all negative excursions of the electrical OFDM waveform below the mean level. This is equivalent to having zero bias on the waveform, so that only positive voltage signals are mapped onto positive optical intensity.

The graph of the BER as a function of the OSNR of this case in shown in figure 4.8.

4.2.2 DHT results

In order to compare the performance of the proposed system based on the Hartley transform, with asymmetrically clipped and DC-biased O-OFDM systems based on FFT presented by other authors [3] [12], the same assumptions will be considered. The impulse response of the optical channel is unitary, and no CP in considered. For the analysis of DC-biased

solution, the performance are evaluate for different bias values. Figure 4.9 shows the BER in function of the optical signal to noise ratio for the DC-biased DHT.

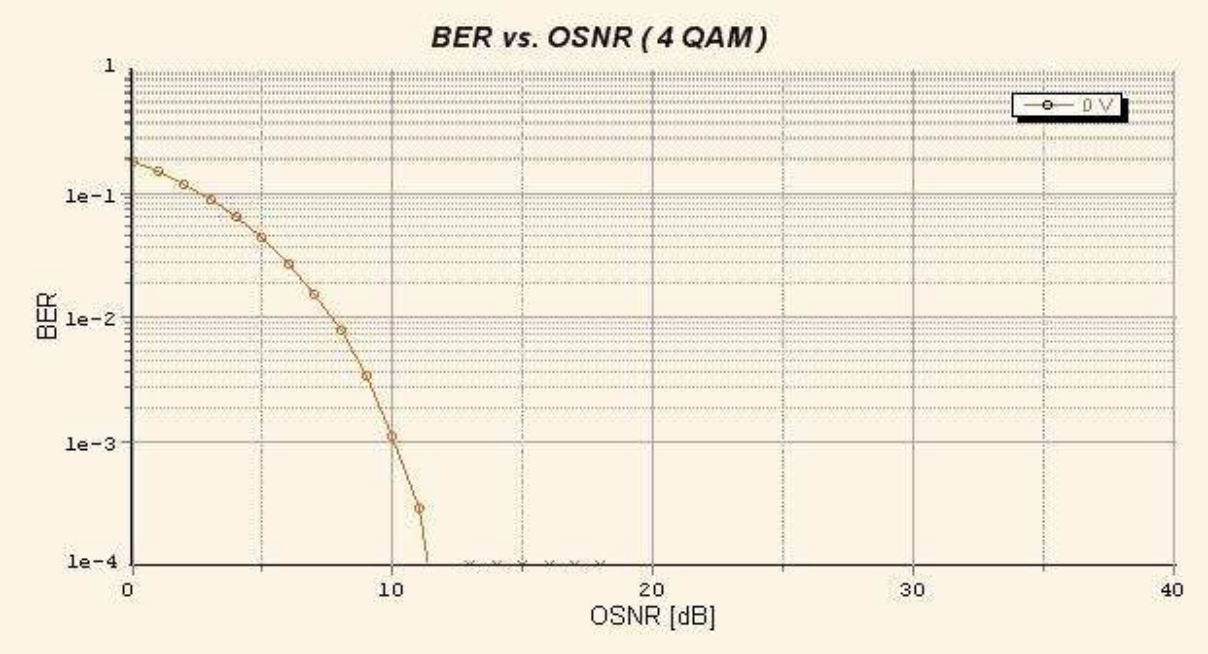

Fig 4.8 – BER as a function of OSNR for the AC-DMT and 4-QAM modulation

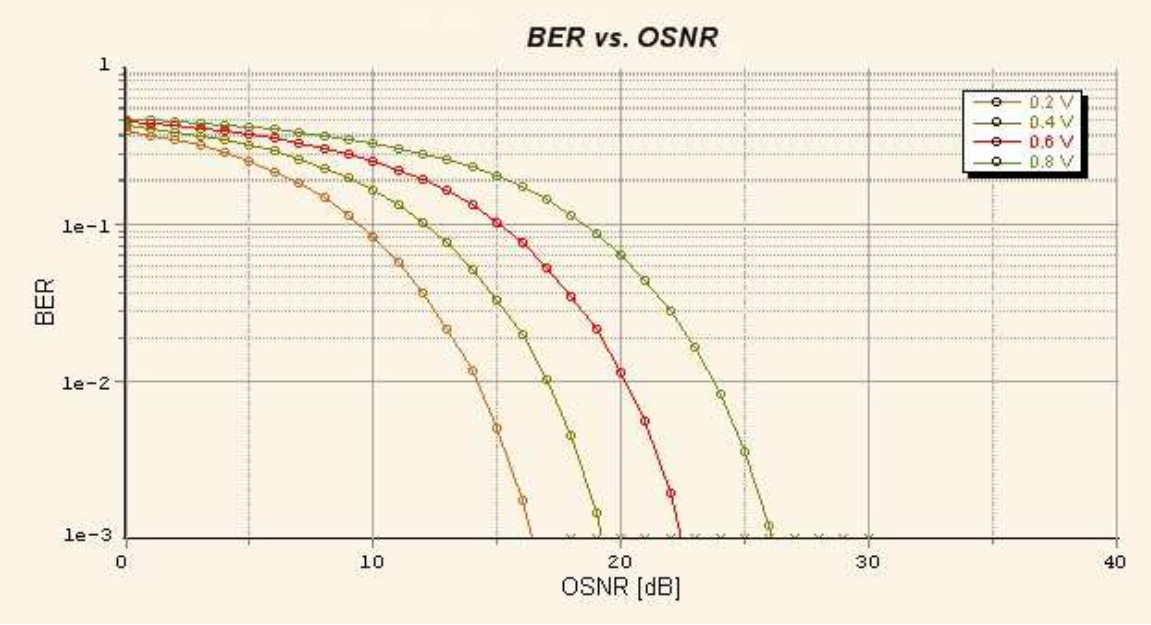

Fig 4.9 - BER as a function of OSNR for the DC-biased DHT and BPSK modulation

ACO-DHT

As it was presented in chapter 3, the Asymmetrically Clipped technique can also be applied to OFDM signals generated by using the Hartley transform. With a suitable choice of the subcarriers to be modulated, the DHT-based OFDM signal can be clipped at zero level and correctly recovered without clipping noise. Figure 4.10 shown the BERvsOSNR graph for a BPSK modulation and same conditions of the previous simulations.

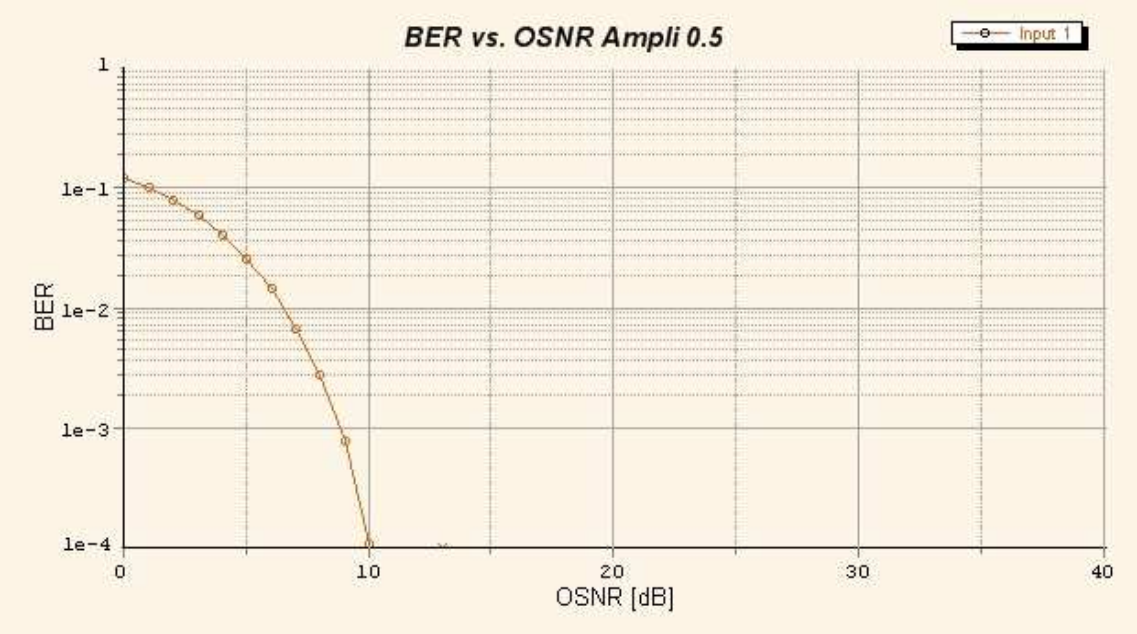

Fig 4.10 - BER as a function of OSNR for the AC DHT and BPSK modulation

Conclusions and future works

This work focus on the study, analysis and the advantages of a power-efficient optical OFDM for Intensity Modulated / Direct Detection systems. As well as being a simple solution to signal dispersion, ACO-OFDM has greater optical efficiency than OOK as demonstrated in [12]. Analytical and simulation results show that for a given normalized bandwidth ACO-OFDM requires less power than DCO-OFDM for all but the largest constellations. Nevertheless, the performance of DCO-OFDM depends on the bias: a large bias increases the required power, while a low bias results in clipping noise which limits performance. For ACO-OFDM the same design is optimum for all constellation sizes, making ACO-OFDM better suited to adaptive systems.

In the second part of this work, the use of the Hartley transform was studied and analyzed: compared to FFT algorithms for real-valued sequence, FHT only requires few more additions. Moreover, the direct and inverse transforms are equal, so that the same fast algorithm can be applied and the same DSP is required for the OFDM modulation and

demodulation. If a real constellation is used, the DHT-OFDM symbols are real. One single DAC and one single ADC are required at the transmitter and receiver, as in DMT systems.

It was demonstrated that DHT-based OFDM signals can be asymmetrically clipped without the need of Hermitian symmetry constrain for the input vector. If only the odd subcarriers are modulated, the signal can be correctly recovered and all the clipping noise falls into the even subcarriers. Moreover, the computational time required to evaluate the complex conjugate of the input constellation symbols vector can be saved. Therefore, the proposed optical OFDM system furnishes a simplified scheme with the same power efficiency of FFT-based ACO-OFDM, resulting suitable for IM/DD optical systems. The analyzed performance shows that the same BER curves, obtained with FFT-based O-OFDM, can be obtained with the proposed O-OFDM scheme based on DHT. With a DHT of the same order and using a real constellation with lower size, the same data sequence at the same bit rate can be transmitted, adopting either DC-biased or ACO solutions.

Future work

The system analyzed is a simple back-to-back system: the next step is verify the impact of the OFDM based on the Discrete Hartley Transform on a fiber link. Adding a link means take into account all the fiber losses and distortions, adding a Cyclic Prefix and equalize the signal.

Equalization

Figures 5.1 and 5.2 show the equalized and unequalized constellation for an OFDM system with 300 m of multimode fiber. Is reasonable to think that the same effects will appear in a DHT system without equalization.

Cyclic Prefix

Although the CP introduces some redundancy, and reduces the overall data rate, it was shown that the use of the CP eliminates both ISI and

inter-carrier interference (ICI) from the received signal and that is the key to simple equalization in OFDM.

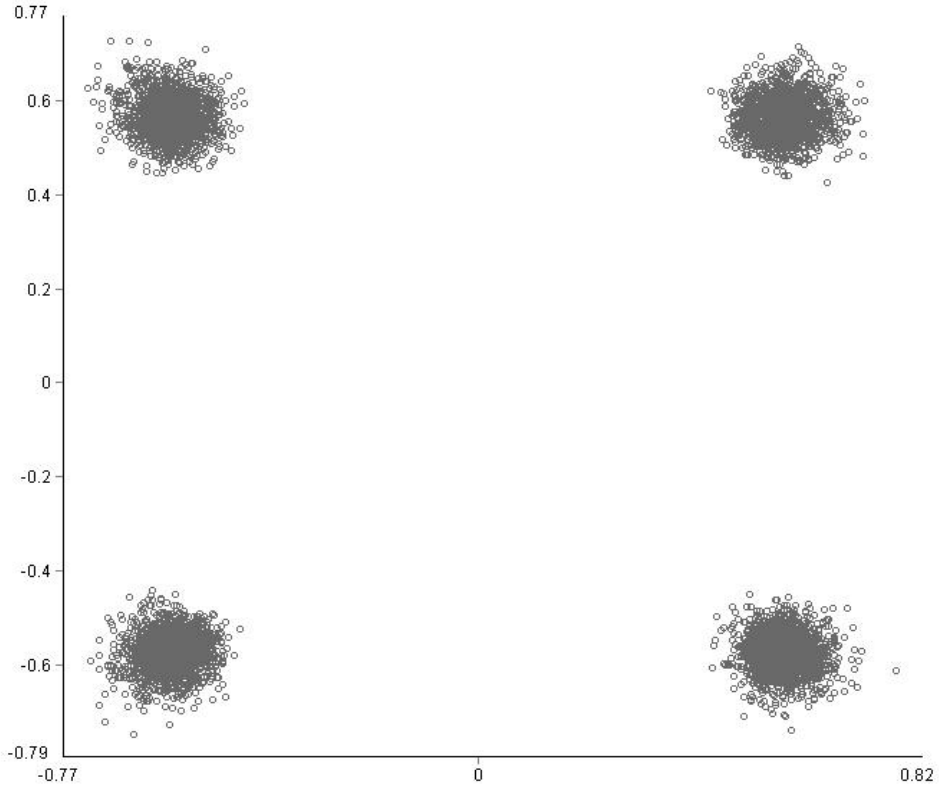

Fig 5.1 Equalized constellation for an OFDM system

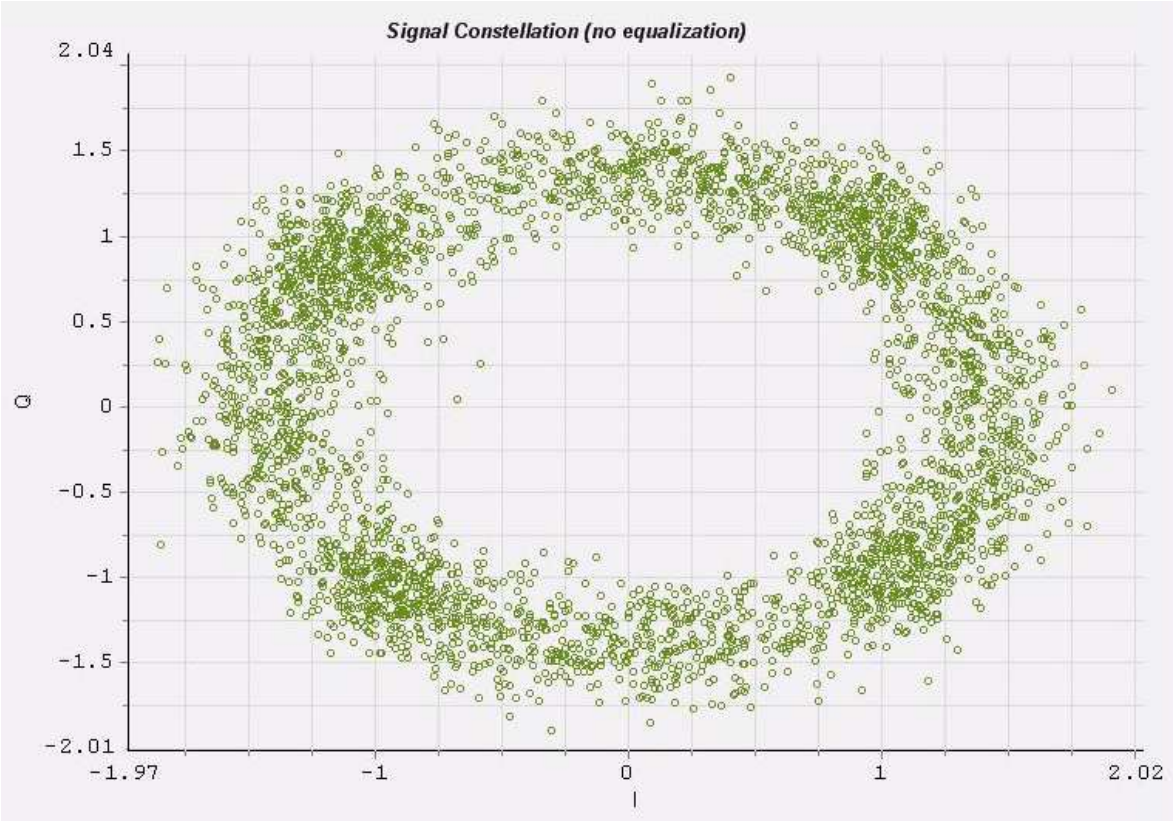

Fig. 5.2 Unequalized constellations for an OFDM system.

Bibliografy

1. J. S. Chow, J. C. Tu, and J. M. Cioffi, "A discrete multitone transceiver system for HDSL applications," *IEEE J. Sel. Areas Commun.*, vol. 9, pp. 895–908, 1991

2. J. Armstrong and A. J. Lowery, "Power efficient optical OFDM," *Electron. Lett.*, vol. 42, pp. 370–371, 2006

3. J. Armstrong and B. J. C. Schmidt, "Comparison of asymmetrically clipped optical OFDM and DC-biased optical OFDM in AWGN," *IEEE Commun. Lett.*, vol. 12, pp. 343–345, 2008

4. X. Li, R. Mardling, and J. Armstrong, "Channel capacity of IM/DD optical communication systems and of ACO-OFDM," in *Proc. ICC '07*, 2007, pp. 2128–2133

5. S. C. J. Lee, F. Breyer, S. Randel, M. Schuster, J. Zeng, F. Huiskens, H. P. A. van den Boom, A. M. J. Koonen, and N. Hanik, "24-Gb/s transmission over 730 m of multimode fiber by direct modulation of 850-nm VCSEL using discrete multi-tone modulation," presented at the Proc. OFC/NFOEC 2007, Anaheim, CA, Mar. 25–29, 2007, Paper PDP6

6. M. Cioffi. (2008, June) A Multicarrier Primer. [Online]. Available: http://www.stanford.edu/group/cioffi/documents/multicarrier.pdf

7. J. Armstrong, "OFDM for Optical Communications," IEEE/OSA Journal of Lightwave Technology, vol. 27, no. 3, pp. 189{204, Feb.1, 2009.

8. S. C. J. Lee, F. Breyer, S. Randel, H. P. A. van den Boom, and A. M. J. Koonen, "High-Speed Transmission over Multimode Fiber using Discrete Multitone Modulation," OSA Journal of Optical Networking, vol. 7, no. 2, pp. 183-196 2008

9. A. J. Lowery and J. Armstrong, "10 Gbit/s multimode fiber link using power-efficient orthogonal-frequency-division multiplexing," *Optics Express*, vol. 13, pp. 10003-10009, 2005

10. R. N. Bracewell, "Discrete Hartley transform," *J. Opt. Soc. Amer.*, vol. 73, pp. 1832–1835, Dec. 1983

11. A. J. Lowery and J. Armstrong, "Comparison of power-efficient optical orthogonal frequency division multiplexing transmission methods," presented at the Conf. Optical Fibre Technology/Australian Optical Society, Melbourne, Australia, Jul. 2006.

12. J. Armstrong, B. J. C. Schmidt, D. Kalra, H. A. Suraweera, and A. J. Lowery, "Performance of asymmetrically clipped optical OFDM in AWGN for an intensity modulated direct detection system," in *Proc. IEEE Global Telecommun. Conf.*, 2006, pp. 1–5

13. R. W. Chang, "Orthogonal Frequency Multiplex Data Transmission System," USA U.S. Patent 3,488,445, 1966.

14. J. Salz and S. B. Weinstein, "Fourier transform communication system," in *Proc. ACM Symp. Problems Optim. Data Commun. Syst.*, Pine Mountain, GA, USA, 1969.

15. A. Peled and A. Ruiz, "Frequency domain data transmission using reduced computational complexity algorithms," in *Proc. ICASSP 80*, Denver, CO, USA, 1980, vol. III, pp. 964–967, IEEE.

16. L. J. Cimini, Jr., "Analysis and simulation of a digital mobile channel using orthogonal frequency division multiplexing," *IEEE Trans. Commun.*, vol. CM-33, pp. 665–675, 1985.

17. R. Lassalle and M. Alard, "Principles of modulation and channel coding for digital broadcasting for mobile receivers," *EBU Tech. Rev.*, pp. 168–190, 1987.

18. J. Armstrong, "OFDM for Optical Communications", JOURNAL OF LIGHTWAVE TECHNOLOGY, VOL. 27, NO. 3, FEBRUARY 1, 2009

19. J. M. Kahn and J. R. Barry, "Wireless infrared communications," *Proc. IEEE*, vol. 85, pp. 265–298, 1997.

20. N. Cvijetic, D. Qian, and T. Wang, "10 Gb/s free-space optical transmission using OFDM," presented at the Proc. OFC/NFOEC 2008, San Diego, CA, 2008, Paper, OTHD2.

21. S. C. J. Lee, F. Breyer, S. Randel, O. Ziemann, H. P. A. van den Boom, and A. M. J. Koonen, "Low-cost and robust 1-Gbit/s plastic optical fiber link based on light-emitting diode technology," presented at the Proc. OFC/NFOEC 2008, San Diego, CA, 2008, Paper, OWB3.

22. J. Armstrong, "Analysis of new and existing methods of reducing intercarrier interference due to carrier frequency offset in OFDM," *IEEE Trans. Commun.*, vol. 47, pp. 365–369, 1999.

23. Y. Li and L. J. Cimini, Jr., "Bounds on the interchannel interference of OFDM in time-varying impairments," *IEEE Trans. Commun.*, vol. 49, pp. 401–404, 2001.

24. A. Garcia Armada, "Understanding the effects of phase noise in orthogonal frequency division multiplexing (OFDM)," *IEEE Trans. Broadcasting*, vol. 47, pp. 153–159, 2001.

25. J. M. Tang, K. Alan Shore, "30-Gb/s Signal Transmission Over 40-km Directly Modulated DFB-Laser-Based Single-Mode-Fiber Links Without Optical Amplification and Dispersion Compensation", JOURNAL OF LIGHTWAVE TECHNOLOGY, VOL. 24, NO. 6, JUNE 2006

26. O. Gonzalez, R. Perez-Jimenez, S. Rodriguez, J. Rabadan, and A. Ayala,"OFDM over indoor wireless optical channel," *Optoelectronics, IEE Proceedings*, vol. 152, pp. 199-204, 2005.

27. Michela Svaluto Moreolo, Raül Muñoz, Gabriel Junyent, "Novel Power Efficient Optical OFDM Based on Hartley Transform for Intensity-Modulated Direct-Detection Systems", JOURNAL OF LIGHTWAVE TECHNOLOGY, VOL. 28, NO. 5, MARCH 1, 2010

28. R. N. Bracewell, "Discrete Hartley transform," *J. Opt. Soc. Amer.*, vol. 73, pp. 1832–1835, Dec. 1983

29. D.Wang, D. Liu, F. Liu, and G. Yue, "A novel DHT-based ultra-wideband system," in *Proc. ISCIT 2005*, Jun. 2004, vol. 50, pp. 172–184

30. B. J. C. Schmidt, A. J. Lowery, and J. Armstrong, "Experimental demonstration of 20 Gbit/s direct-detection optical OFDM and 12 Gbit/s with a colorless transmitter," presented at the Optical Fiber Communication Conf. 2007, Anaheim, CA, Mar. , Paper PDP 18